Photo-responsive chemistries for user-defined hydrogel network modulation to investigate cell-matrix interactions

Journal:	*Accounts of Chemical Research*
Manuscript ID	Draft
Manuscript Type:	Article
Date Submitted by the Author:	n/a

Complete List of Authors:	Hushka, Ella; University of Colorado Boulder, Chemical and Biological Engineering; University of Colorado Boulder BioFrontiers Institute Ohnsorg, Monica; University of Colorado Boulder, Chemical and Biological Engineering; University of Colorado Boulder BioFrontiers Institute Anseth, Kristi; University of Colorado Boulder, Chemical and Biological Engineering; University of Colorado Boulder BioFrontiers Institute

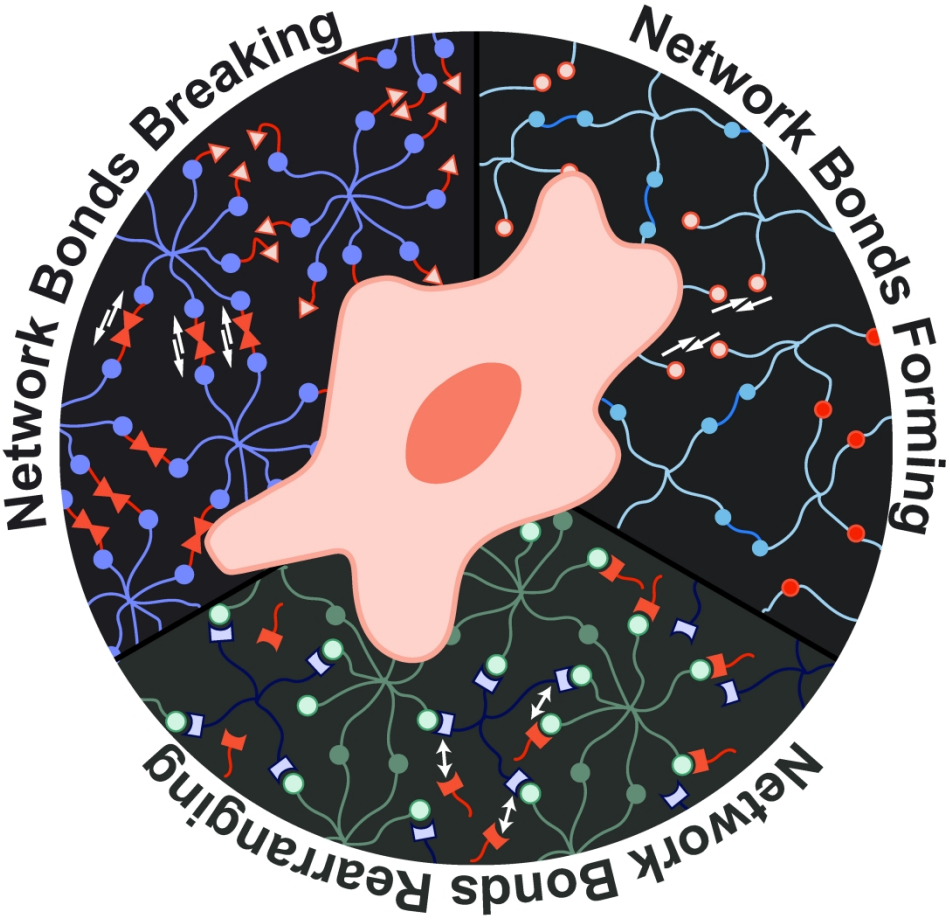

Table of Contents Figure

326x312mm (300 x 300 DPI)

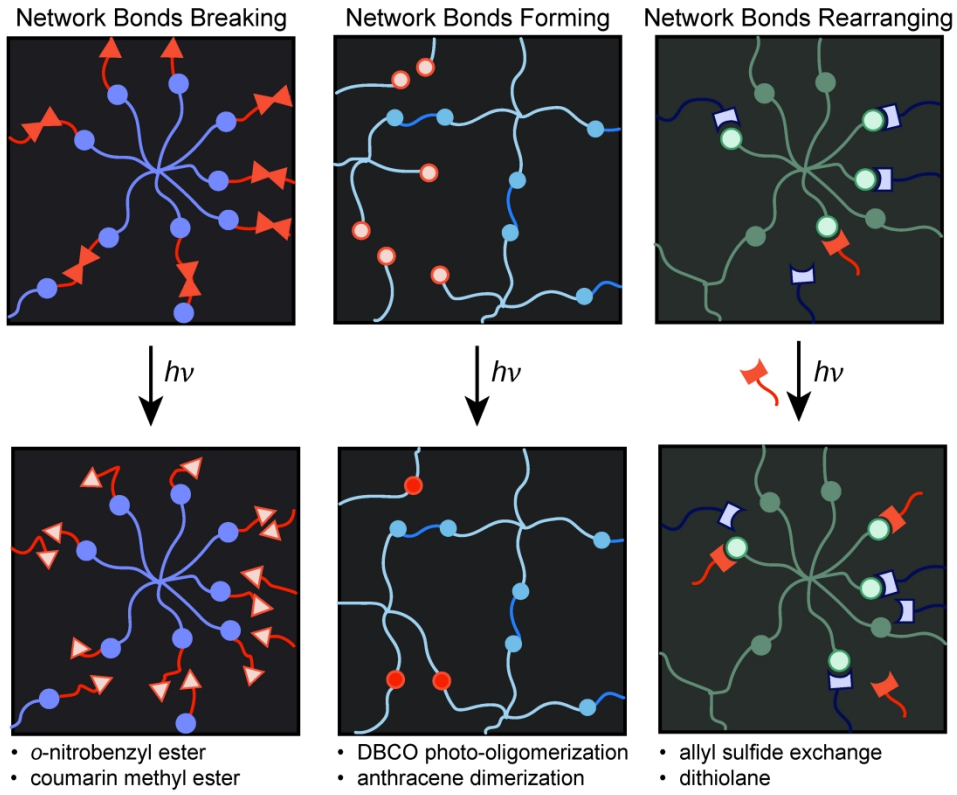

Figure 1. "Chemical Toolbox" for light-mediated hydrogel network transformations. Network a) bond breaking – using light to cleave bonds within the network (solid orange triangles to open orange triangles), b) bond formation – using photoactive moieties to introduce additional crosslinks within the network (open orange circles to solid orange circles), and c) bond rearrangement – using photolabile moieties to exchange bonds within the network (exchange of network incorporated blue moieties with monofunctional orange moieties).

314x265mm (300 x 300 DPI)

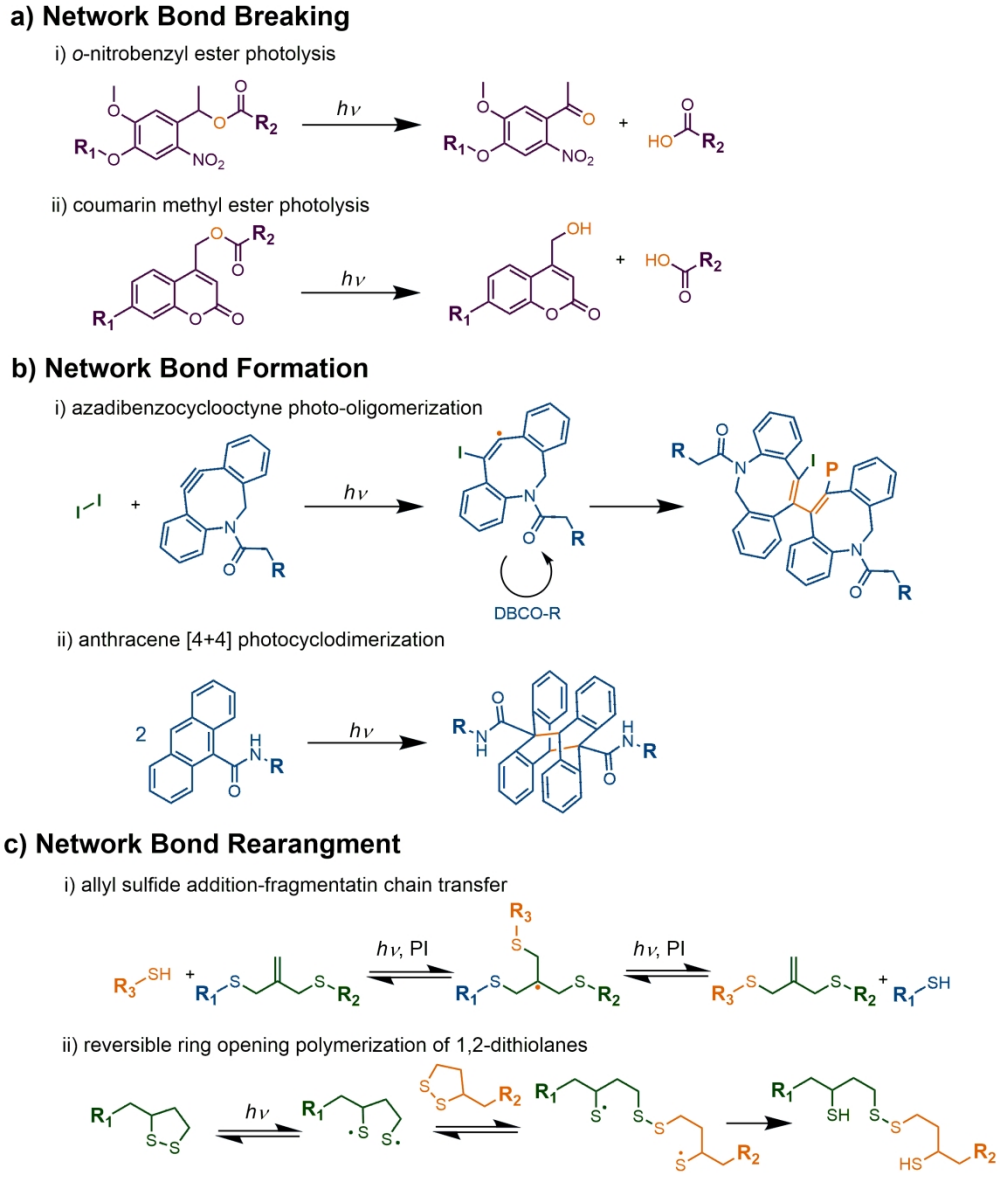

Scheme 1. Schemes of photo-chemical transformations within hydrogel networks. a) Bond breaking (i) *o*-nitrobenzyl ester and (ii) coumarin methyl ester; b) bond formation (i) DBCO photo-oligomerization (ii) anthracene dimerization; c) bond rearrangements (i) allyl sulfide exchange and (ii) 1,2-dithiolanes.

207x244mm (300 x 300 DPI)

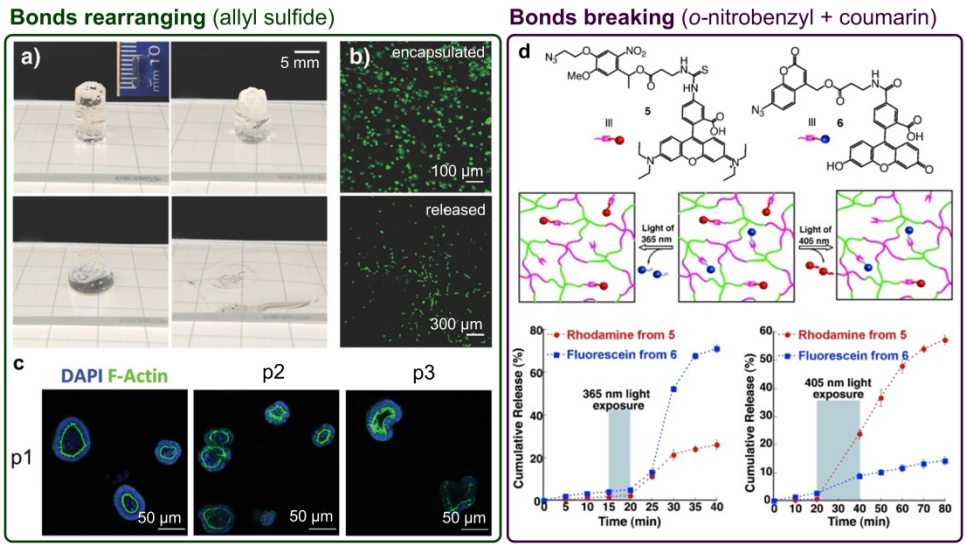

Figure 2. Photodegradation: cell harvesting to release biomolecules. a) Amplified photodegradation of a hydrogel with AIS crosslinks b) viability of human MSCs before and after AIS photodegradation (adapted with permission from ref. (26), Copywrite 2017 Wiley-VCH). c) Murine intestinal organoids passaged using photodegradable AIS hydrogels through passage 3 (adapted with permission from ref. (31), Copywrite 2020 Wiley-VCH) d) Sequential release of rhodamine (red) and fluorescein (blue) using the excitation wavelengths 405 nm for *o*-Nb and 365 nm for coumarin methyl ester photolysis (adapted with permission from ref. (36), Copywrite 2013 Wiley-VCH).

223x126mm (600 x 600 DPI)

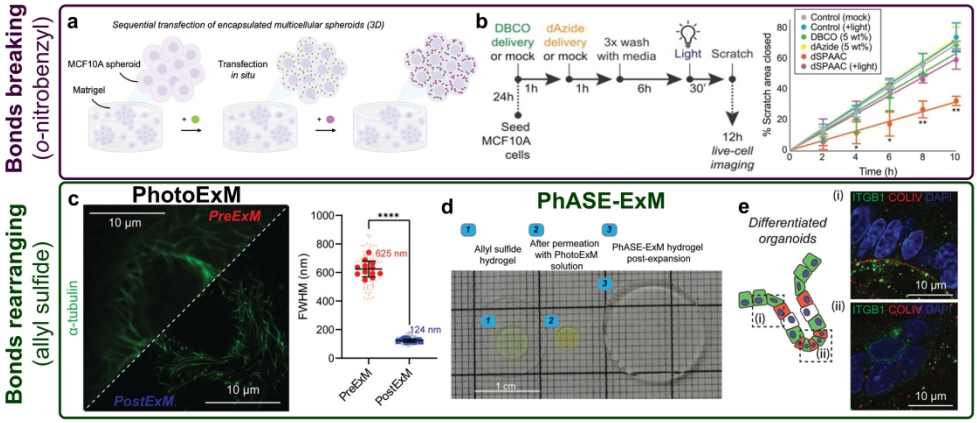

Figure 3. Photodegradation: applications in biostasis and imaging. a) Illustration of how the photodegradable SPAAC network is transfected within cells to slow intracellular processes. (adapted with permission from ref. (39), Copywrite 2023 Wiley-VCH). b) Timeline of biostasis transfection showing reduced cell migration with SPAAC treatment (orange) and recovered cell proliferation and migration following light exposure to degrade the o-Nb moieties and reverse intracellular gelation (pink). (adapted with permission from ref. (38), Copywrite 2022 Wiley-VCH). c) α-tubulin imaging pre- and post-expansion demonstrating the improvement in resolution using the full width half max (FWHM) of microtubule diameter (**** p<0.0001). d) Visual depiction of hydrogel swelling after fluorophore transfer. e) PhASE-ExM images showing the organization of integrin β1 and collagen IV within the (i) hinge and (ii) crypt regions of the organoid post-differentiation. (adapted with permission from ref. (1), Copywrite 2022 Wiley-VCH).

218x95mm (600 x 600 DPI)

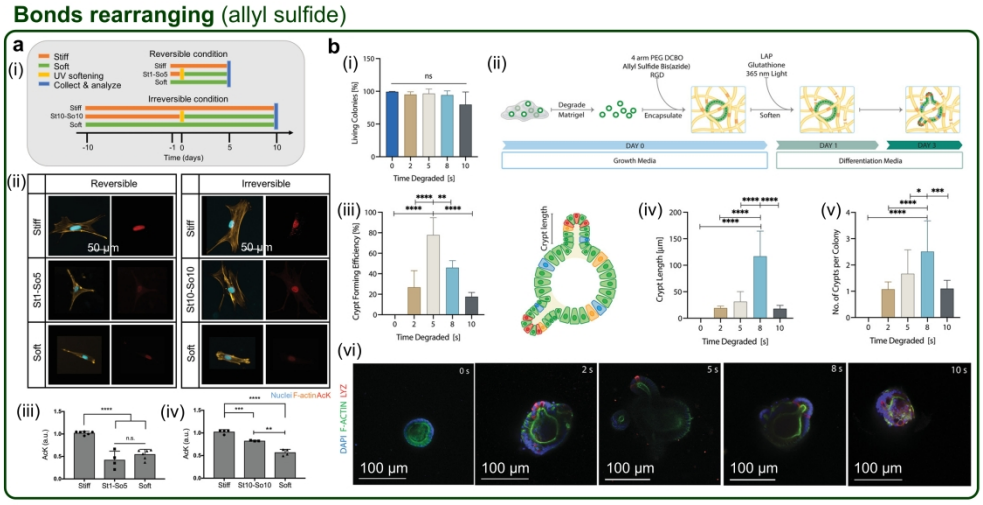

Figure 4. Photo-softening: recovery of stemness and organoid crypt formation. a) (i) Timeline of in situ photo-softening for the reversible and irreversible histone acetylation. (ii) Fluorescence images showing the reversible and irreversible nuclear localization of AcK on the left and right, respectively. Quantification of AcK intensity in (iii) reversible and (iv) irreversible conditions. (adapted with permission from ref. (2), Copywrite 2018 Wiley-VCH). b) (i) Organoids remained viable under 10 seconds of light irradiation. (ii) Schematic detailing the encapsulation, growth, photo-softening, and differentiation timeline for intestinal organoids within AIS hydrogels. Quantification of (iii) crypt forming efficiency, (iv) crypt length, and (v) number of crypts per colony to identify the optimal time of light irradiation for organoid differentiation with corresponding (vi) fluorescence images. (adapted with permission from ref. (50), Copywrite 2020 Wiley-VCH).

218x114mm (600 x 600 DPI)

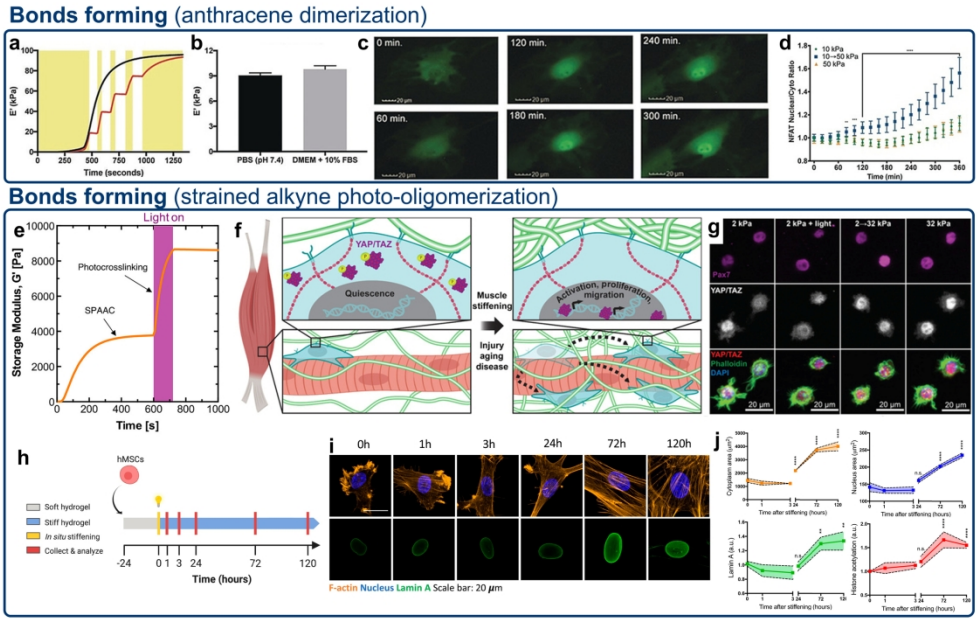

Figure 5. Photo-stiffening: from investigating mechanobiology to modeling diseased tissues. a) *In situ* gelation of the PEG-anthracene hydrogel with continuous light (black) or pulsed light (red). b) Comparison of modulus after gelation in PBS vs. DMEM + 10% FBS. c) Fluorescence images showing the nuclear translocation of NFAT over 300 minutes and d) quantification of the nuclear/cytoplasmic ratio of NFAT under static or transient stiffening (blue, square) (adapted with permission from ref. (21), Copywrite 2019 Wiley-VCH). e) Photo-stiffening post-network formation via DBCO photo-oligomerization under light irradiation (adapted with permission from ref. (20), Copywrite 2018 American Chemical Society). f) Illustration demonstrating how the nuclear translocation of YAP/TAZ is indicative of injury, aging, and disease in muscle cells. g) Fluorescence images depicting the nuclear translocation of YAP/TAZ (grey) after substrate stiffening (2 → 32 kPa). (adapted with permission from ref. (3), Copywrite 2021 Wiley-VCH) h) Timeline of experiment to test the effect of *in situ* stiffening. i) Fluorescence images showing the increasing intensity of Lamin A in the nucleus with time after network stiffening. j) Quantification of the cytoplasmic area (yellow), nucleus area (blue), Lamin A intensity (green) and histone acetylation intensity (red) with time after stiffening. (adapted with permission from ref. (56), Copywrite 2020 National Academy of Sciences).

220x142mm (300 x 300 DPI)

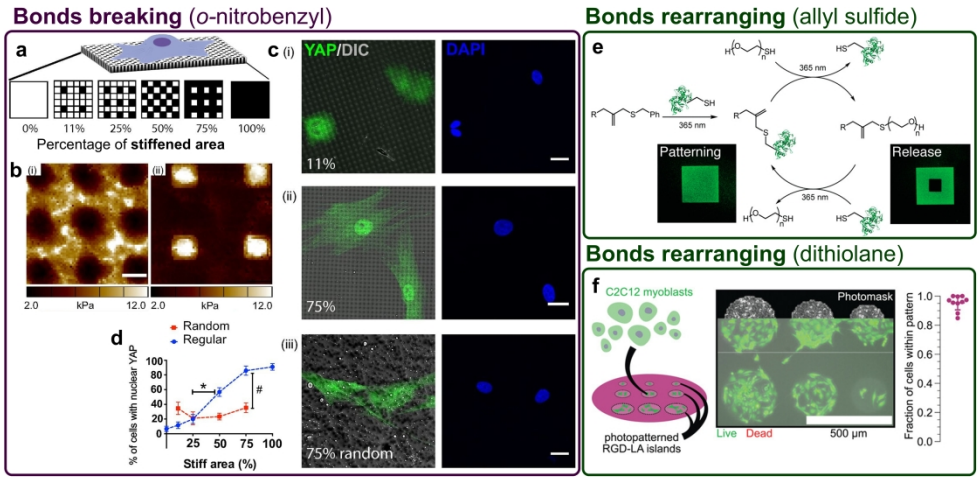

Figure 6. 2D Precision patterning to control cell-substrate interactions. a) Photodegraded surfaces with different percentages of stiff area. b) Atomic force microscopy images of the (i) 75% and (ii) 11% stiff conditions. c) Fluorescent and differential interference contrast (DIC) images showing the nuclear translocation of YAP across the (i) 11% stiff, regular, (ii) 75% stiff, regular, and (iii) 75% stiff, random substrates. d) Percentage of cells with nuclear YAP across increasing total stiff areas between regular (blue) and randomly (red) patterned substrates. (adapted with permission from ref. (60), Copywrite 2016 National Academy of Science). e) Circular patterning and release cycle of biomolecules using AlS exchange reactions (adapted with permission from ref. (24), Copywrite 2018 American Chemical Society). f) Photopatterned regions of lipoic acid functionalized RGD (RGD-LA) to spatially pattern the adherence of C2C12 myoblasts (adapted with permission from ref. (29), Copywrite 2023 Wiley-VCH).

219x109mm (600 x 600 DPI)

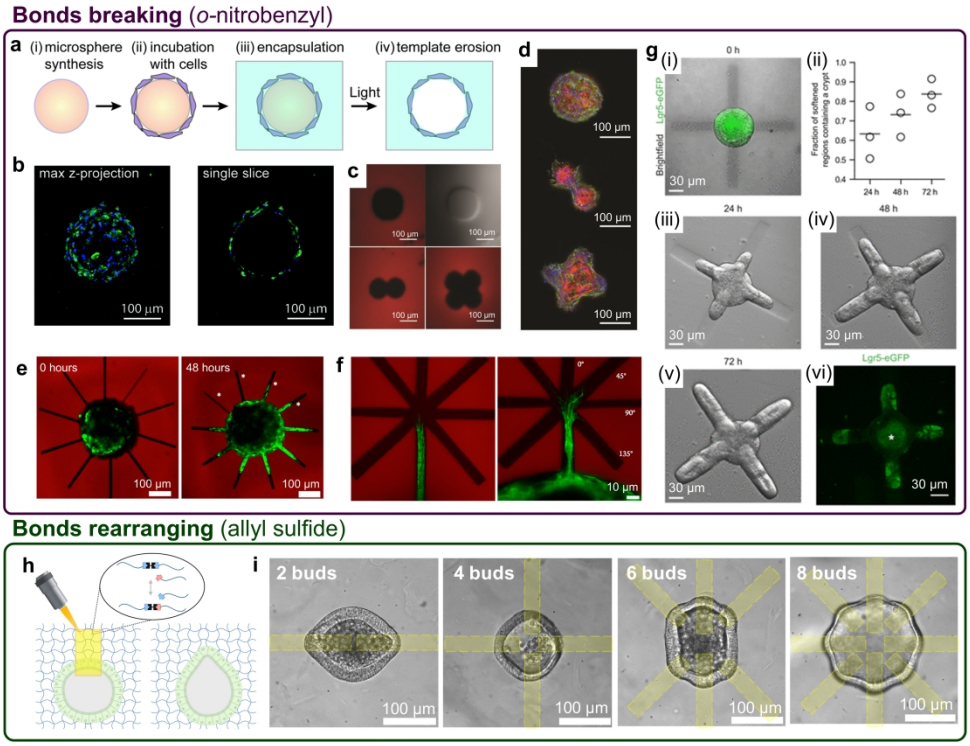

Figure 7. Photo-patterning to enable morphogenesis of multicellular constructs. a) Illustration of lung alveoli patterning process around microspheres, encapsulation, and subsequent photodegradation. b) Fluoresces images of a templated lung alveoli and a cross-section showing the hollow core. (adapted with permission from ref. (69), Copywrite 2015 Royal Society of Chemistry). c) Photopatterned wells for lung alveoli with 1, 2, and 4 lobes. d) Successful culture of lung alveoli within the patterned wells (adapted with permission from ref. (70), Copywrite 2014 Oxford University Press). e) Encapsulated neurosphere with eroded channels immediately and 48 hours after patterning. Channels marked with an asterisk were not completely eroded. f) Fork-shaped patterns before (left) and after (right) the axons reached the fork showing preferred directionality at 45°. (adapted with permission from ref. (71), Copywrite 2014 American Chemical Society). g) (i) photodegraded cross structure around a spherical intestinal organoid (green, stem cells, Lgr5+). (ii) Quantification of the percentage of patterned region that is filled by the organoid over (iii) 24, (iv) 48, and (v) 72 hours after patterning. (vi) Fluorescence image showing the migration of Lgr5+ stem cells to the ends of the patterned crypts. Asterisk denotes autofluorescence of the dead cells shed into the organoid core (adapted with permission from ref. (48), Copywrite 2022 AAAS). h) Illustration light induced viscoelasticity to pattern regions around an encapsulated intestinal colony. i) Brightfield images of patterned organoids deforming into the patterned regions with 2-8 buds after patterning. (adapted with permission from ref. (4), Copywrite 2023 AAAS).

218x166mm (600 x 600 DPI)

Photo-responsive chemistries for user-directed hydrogel network modulation to investigate cell-matrix interactions

Ella A. Hushka[1,2,=], Monica L. Ohnsorg[1,2,=], and Kristi S. Anseth[1,2]

[1]Department of Chemical and Biological Engineering, University of Colorado Boulder, Boulder, CO, 80303 USA

[2]BioFrontiers Institute, University of Colorado Boulder, Boulder, CO, 80303 USA

[=] *these authors contributed equally*

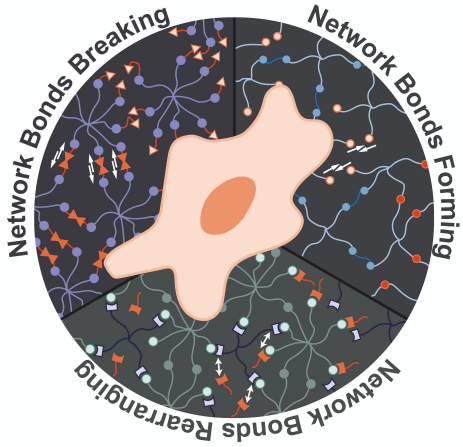

Conspectus:

Synthetic extracellular matrix (ECM) engineering is a highly interdisciplinary field integrating materials and polymer science and engineering, chemistry, cell biology, and medicine to develop innovative strategies to investigate and control cell-matrix interactions. Cellular microenvironments are complex and highly dynamic – changing in response to injury and disease. To capture some of these critical dynamics *in vitro*, biomaterial matrices have been developed with tailorable properties that can be modulated *in situ* in the presence of cells. While numerous macromolecules can serve as a basis in the design of a synthetic ECM, our group has exploited multi-arm poly(ethylene glycol) (PEG) macromolecules because of the ease of functionalization, many complementary bio-click reactions to conjugate biological signals, and ultimately, the ability to create well-defined systems to investigate cell-matrix interactions. For example, significant strides have been made in developing bio-responsive and transient synthetic ECM materials that degrade, relax stress, or strain-stiffen on cell-dictated time scales. In addition, our group has designed hydrogels incorporating different photo-responsive moieties, and these moieties facilitate user-defined spatiotemporal modulation of the extracellular microenvironment *in vitro*. The application of light allows one to break, form, and rearrange network bonds in the presence of cells to alter the biomechanical and biochemical microenvironment to investigate cell-matrix interactions in real-time. Such photo-responsive materials have facilitated fundamental discoveries in the

biological pathways related to outside-in signaling, which guide important processes related to tissue development, homeostasis, disease progression, and regeneration.

This review focuses on the photo-tunable chemical toolbox that has been used modulate hydrogel properties post-network formation through: bond-breaking chemistries, such as *o*-nitrobenzyl and coumarin methyl ester photolysis; bond-forming chemistries, such as azadibenzocyclooctyne photo-oligomerization and anthracene dimerization; and bond-rearranging chemistries, such as allyl sulfide addition-fragmentation chain transfer and reversible ring opening polymerization of 1,2-dithiolanes. By using light to modulate the cellular microenvironment (in 2D, 3D and even 4D), innovative experiments can be designed to study mechanosensing of single cells or multicellular constructs, pattern adhesive ligands to spatially control cell-integrin binding or modulate on-demand the surrounding cell niche to alter outside-in signaling in a temporally controlled manner. To date, these photochemically defined materials have been used for the culture, differentiation, and directed morphogenesis of primary cells and stem cells, co-cultured cells, and even multicellular constructs (*e.g.,* organoids).

Herein, we present examples of how this photochemical toolbox has been used under physiological reaction conditions with spatiotemporal control to answer important biological questions and address medical needs. Specifically, our group has exploited these materials to study mesenchymal stem cell mechanosensing and differentiation, the activation of fibroblasts in the context of valve and cardiac fibrosis, muscle stem cell response to matrix changes during injury and aging, and predictable symmetry breaking during intestinal organoid development. The materials and reactions described herein are diverse and enable the design and implementation of an array of hydrogels that can serve as cell delivery systems, tissue engineering scaffolds, or even *in vitro* models for studying disease or screening for new drug treatments.

Key References:

- Blatchley, M. R.; Günay, K. A.; Yavitt, F. M.; Hawat, E. M.; Dempsey, P. J.; Anseth, K. S. In Situ Super-Resolution Imaging of Organoids and Extracellular Matrix Interactions via Phototransfer by Allyl Sulfide Exchange-Expansion Microscopy (PhASE-ExM). *Adv. Mater.* **2022**, *34* (16), 2109252. https://doi.org/10.1002/adma.202109252.[1] *This work highlights a novel use of allyl sulfide-mediated bond rearranging reactions to enable increased imaging resolution.*
- Killaars, A. R.; Grim, J. C.; Walker, C. J.; Hushka, E. A.; Brown, T. E.; Anseth, K. S. Extended Exposure to Stiff Microenvironments Leads to Persistent Chromatin Remodeling in Human Mesenchymal Stem Cells. *Adv. Sci.* **2019**, *6* (3), 1801483. https://doi.org/10.1002/advs.201801483.[2] *This paper outlines the*

role of nuclear mechanosensing in stem cell regenerative potential and when that potential is lost versus recovered.

- Silver, J. S.; Günay, K. A.; Cutler, A. A.; Vogler, T. O.; Brown, T. E.; Pawlikowski, B. T.; Bednarski, O. J.; Bannister, K. L.; Rogowski, C. J.; Mckay, A. G.; DelRio, F. W.; Olwin, B. B.; Anseth, K. S. Injury-Mediated Stiffening Persistently Activates Muscle Stem Cells through YAP and TAZ Mechanotransduction. *Sci. Adv.* **2021**, *7* (11), eabe4501. https://doi.org/10.1126/sciadv.abe4501.[3] *This demonstration of in situ photo-stiffening through strained alkyne photo-oligomerization shows how hydrogel microenvironments can be tuned to mimic muscle injury.*
- Yavitt, F. M.; Kirkpatrick, B. E.; Blatchley, M. R.; Speckl, K. F.; Mohagheghian, E.; Moldovan, R.; Wang, N.; Dempsey, P. J.; Anseth, K. S. In Situ Modulation of Intestinal Organoid Epithelial Curvature through Photoinduced Viscoelasticity Directs Crypt Morphogenesis. *Sci. Adv.* **2023**, *9* (3), eadd5668. https://doi.org/10.1126/sciadv.add5668.[4] *This work elucidates the way patterned, photoinduced viscoelasticity can promote epithelial curvature that templates crypt formation in intestinal organoids cultured in an allyl sulfide containing hydrogel.*

I. Introduction:

In vivo, cells reside in a tissue specific extracellular matrix (ECM) with a rich milieu of signals that dynamically change during development, disease progression, or after injury. These spatiotemporal changes include both biomechanical and biochemical signals that alter cellular functions in 3D and with time (i.e., 4D). To mimic the ECM, bioengineers have developed a range of synthetic hydrogels, broadly used to culture cells in 4D for applications in tissue engineering, stem cell and organoid differentiation, and regenerative medicine.[5–8] Many of these hydrogels include moieties that facilitate transient network properties such as degradation, stress-relaxation,[9–11] or strain-stiffening[12] on cell-dictated time scales, as well as stimuli-responsive moieties, which allow the user to recapitulate dynamic changes of the ECM microenvironment towards better *in vitro* models of *in vivo* processes. These uses of bio-orthogonal chemical functional groups allow scientists to introduce biochemical signals and modulate the biomechanical properties of synthetic hydrogels globally, locally, temporally, and consecutively to study how cells respond to altered matrix cues in a controlled 3D microenvironment.

In this Account, we highlight some of the recent work of the Anseth group to advance ECM engineering through the synthesis and design of dynamic, photo-tunable hydrogels. A suite of chemistries has been developed that allows user-defined control over hydrogel properties with light and can be optimized for specific biological questions and applications.[5,13] Here, we highlight how *o*-nitrobenzyl ester *(o*-Nb*),* coumarin methyl ester,

azadibenzocyclooctyne (DBCO), anthracene, allyl sulfide (AlS), and 1,2-dithiolane moieties can be utilized with increasing levels of user control – from bulk property modifications to precise patterning – to make fundamental advancements in understanding cell-matrix interactions, mechanosensing, and outside-in signaling. With these chemistries, we demonstrate the applications of post-network formation modifications through controlled bond-breaking, -forming, and -rearranging events with spatiotemporal precision, all in the presence of single cells or multicellular structures.

II. Chemical Toolbox for Photo-tunable Network Transformations:

Photo-click and photochemical reactions for network formation have been extensively reviewed by Anseth, Bowman, and coworkers.[13,14] In this Account, we focus on covalently crosslinked hydrogels and the use of light-mediated chemical transformations to induce network bond breaking (Figure 1a), formation (Figure 1b), and rearrangements (Figure 1c) in the presence of living cells. Specifically, we describe the chemical toolbox that can be drawn from to create cell-laden, photo-tunable hydrogels with desired material properties that capture key aspects of the ECM, called synthetic ECM mimics.

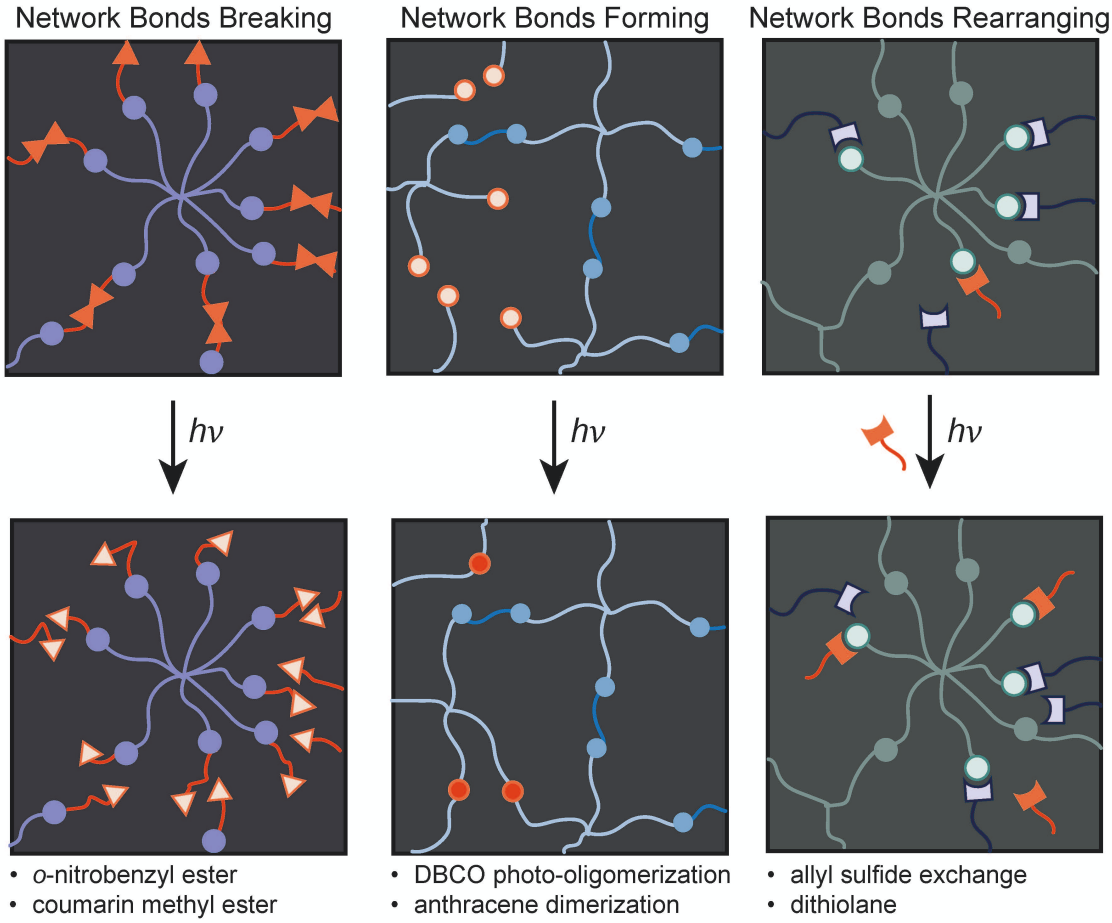

Figure 1. "Chemical Toolbox" for light-mediated hydrogel network transformations. Network a) bond breaking – using light to cleave bonds within the network (solid orange triangles to open orange triangles), b) bond formation – using photoactive moieties to introduce additional crosslinks within the network (open orange circles to solid orange circles), and c) bond rearrangement – using photolabile moieties to exchange bonds within the network (exchange of network incorporated blue moieties with monofunctional orange moieties).

2.1. o-Nitrobenzyl Ester and Coumarin Methyl Ester Photolysis (bonds breaking)

Cleaving bonds upon light exposure leads to a decrease in the network cross-linking density or even complete network erosion, allowing one to spatiotemporally modulate hydrogel properties such as modulus, water content, and diffusivity.[15,16] Two photolytic chemistries, *o*-Nb (Scheme 1a, i) and coumarin methyl ester (Scheme 1a, ii), are used extensively by our group. Crosslink cleavage with light results in efficient network degradation.[17] The photolytic efficiency of the *o*-Nb-derived moiety using low intensity flood light exposure and either single or multi-photon excitation using a laser scanning confocal microscope (365 nm or 405 nm) allows for bulk and precision network degradation, respectively, through bond cleavage into nitroso- and acid-terminated byproducts (Scheme 1a,i).[18] Coumarin methyl ester moieties in hydrogels enable the use of ultraviolet to visible wavelengths of light, 315 – 860 nm, to induce bond scission events (Scheme 1a, ii).[19]

2.2. Strained Alkyne Photo-oligomerization and Anthracene Dimerization (bonds forming)

Bond formation is the complementary network transformation to bond breaking, which typically leads to increased network crosslinks. This is relevant from a biological standpoint, as tumors and fibrotic disease are characterized by ECM stiffening. To mimic this, we have designed hydrogels with DBCO and anthracene moieties that can be photo-crosslinked and stiffened *in situ* to study cellular mechanosensing (Scheme 1b). Strain-promoted azide-alkyne cycloaddition (SPAAC) click chemistry is a bio-orthogonal reaction that has become ubiquitous as a method to rapidly form well-defined hydrogel networks in the presence of cells. Our group discovered that off-stoichiometry formulations with excess DBCO can undergo a secondary photo-oligomerization reaction in the presence of light and a radical photoinitiator to increase the crosslinking density and network modulus (Scheme 1b,i).[20] A complementary route to prepare photo-stiffening hydrogels, without the need for any exogenously added molecules, is the [4+4] photocyclodimerization of anthracene when irradiated with low intensity 365 nm light (Scheme 1b,ii).[21]

2.3. Allyl Sulfide Addition-Fragmentation Chain Transfer (bonds rearranging)

Chemical transformations that rely on the exchange of reactive moieties provide a robust method to modulate network crosslinking (i.e., covalent adaptable networks) or presentation of pendant functionalities in a *reversible* manner. Building from advancements in chain transfer agents used in reversible-addition fragmentation chain transfer (RAFT) polymerization techniques,[22] AlS moieties incorporated into network crosslinks enable dynamic changes in hydrogel network structure and functionality through photochemically initiated bond exchange. RAFT is facilitated by a thiyl radical, following preliminary initiation from a photoinitator, that propagates through the double bond resulting in an unstable symmetric intermediate that undergoes β-scission resulting in the addition of the attacking thiyl radical and fragmentation of an original pendent group regenerating the double bond (Scheme 1c,i).[23] The induction of this bond rearrangement enables multiple functional outcomes, such as reversible ligand exchange[23,24] and photoinduced viscoelasticity.[25] If monofunctional thiols are introduced during photoinitiated exchanges, the AlS crosslinks can be consumed, leading to rapid network dissolution (i.e., reverse gelation) due to amplification of the monothyil radicals.[26]

2.4. Reversible Ring Opening Polymerization of 1, 2-Dithiolanes (bonds rearranging)

Disulfides provide another strategy to integrate radical-mediated photodegradable and photo-adaptable functionality into networks.[27] Recently, we introduced dynamic covalent crosslinks into hydrogel systems using ring-strained disulfides, like 1,2-dithiolanes, which can undergo reversible ring opening polymerization (ROP).[28] These five-membered heterocycles absorb light and can be used to generate thiyl radicals through breaking the disulfide bond and opening the ring with or without photoinitiator (Scheme 1c,ii). The thiyl radicals can

homopolymerize to form linear disulfide crosslinks, or in the presence of photoinitiator and an alkene (e.g., norbornene), the ring-opened dithiolane can add to either side of the alkene creating permanent thioether bonds. By tuning the ratio of 1,2-dithiolane to alkene moieties and free thiols, we have recently demonstrated how the degree of bond re-arrangement and subsequent stress-relaxation in the networks can be controlled in the presence of cells.[29,30]

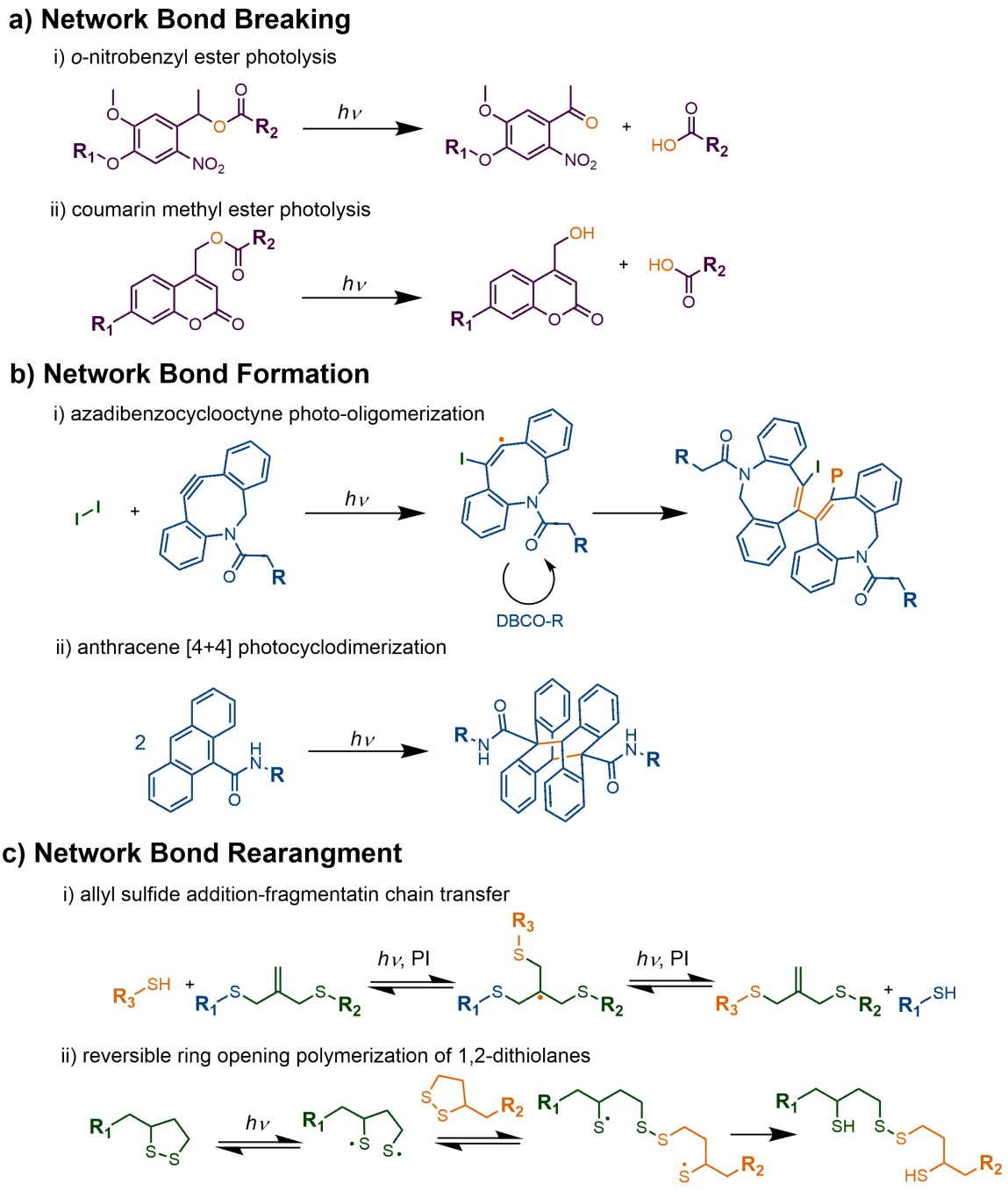

Scheme 1. Schemes of photo-chemical transformations within hydrogel networks. a) Bond breaking (i) *o*-nitrobenzyl ester and (ii) coumarin methyl ester; b) bond formation (i) DBCO photo-oligomerization (ii) anthracene dimerization; c) bond rearrangements (i) allyl sulfide exchange and (ii) 1,2-dithiolanes.

III. Hydrogel Transformations for Cellular Microenvironment Modulation:

The photo-chemical transformations described above enable the modulation of biochemical and biomechanical matrix signals in both time and space in the presence of cells. Thus, these materials enable the study of mechanostransduction and outside-in signaling pathways.

3.1. Photodegradation – Network Bond Breaking and Erosion

The following sections provide examples of how photodegradation has been used to erode cell-laden matrices to recover cells, release tethered biomolecules, reverse biostasis, or obtain high resolution images via expansion microscopy.

3.1. 1. Hydrogel erosion for cell encapsulation and recovery (AlS)

When cells are encapsulated in 3D synthetic ECMs, a more biologically relevant culture environment is achieved, but many assays are more difficult to perform. For example, recovery of encapsulated cells for passaging or advanced biological analyses is challenging. To overcome some of these limitations, AlS-containing hydrogel networks were engineered with rapid degradation kinetics for the recovery of single cells[26] or multicellular intestinal organoids[31] from thick hydrogels (up to 1 cm) (Figure 2a). Addition of a photoinitiator (Lithium phenyl-2,4,6-trimethylbenxoulphosphinate, LAP), glutathione (a monofunctional thiol), and 365 nm light led to an amplified radical-mediated degradation and dissolution in <1 minute, which maintained cell viability and allowed for subsequent cultures of single cells (Figure 2a-b).[26] Photolabile matrices have been used as an alternative to Matrigel, while allowing passaging and maintenance of intestinal organoid colonies. Matrigel is a proteinaceous hydrogel that is widely used for organoid cultures,[32] but it leads to an ill-defined microenvironment and prevents the transplantation of organoids to address clinical needs. As a synthetic ECM alternative, we used AlS-based hydrogels to culture intestinal stem cells (ISCs) for 4 days to efficiently form cystic colonies, at which point the AlS hydrogels were fully photodegraded to release them. The colonies were then dissociated to single ISCs, removing any dead cells, and then re-encapsulated into fresh AlS-based hydrogels (i.e., passaged) (Figure 2c). This process was repeated multiple times to demonstrate robust passaging capabilities.[31] Together, these works demonstrate the advantages of photodegradable hydrogels as 3D culture systems that allow recovery and capture of cells.[26]

3.1. 2. Photolysis of network tethered moieties for tunable release from hydrogels (o-Nb and coumarin)

Photodegradable network tethers have also been used to release pendant moieties for user-directed presentation and delivery of cell signaling molecules (*e.g.,* proteins and integrin binding peptide epitopes).[15,33–35] In one application, multiple cargos are released at staged times by integration of two different photolysis chemistries, *o*-Nb and coumarin methyl ester, which were preferentially photolabile at 405 nm and 365 nm, respectively (Figure 2d). Flood light irradiation was used to individually or sequentially release bioactive growth

factors tethered within the matrix (Figure 2d). Depending on the timing of the irradiation and its wavelength, we were able to pulse the release of BMP-7 versus BMP-2 to manipulate the osteogenic differentiation of MSCs.[36]

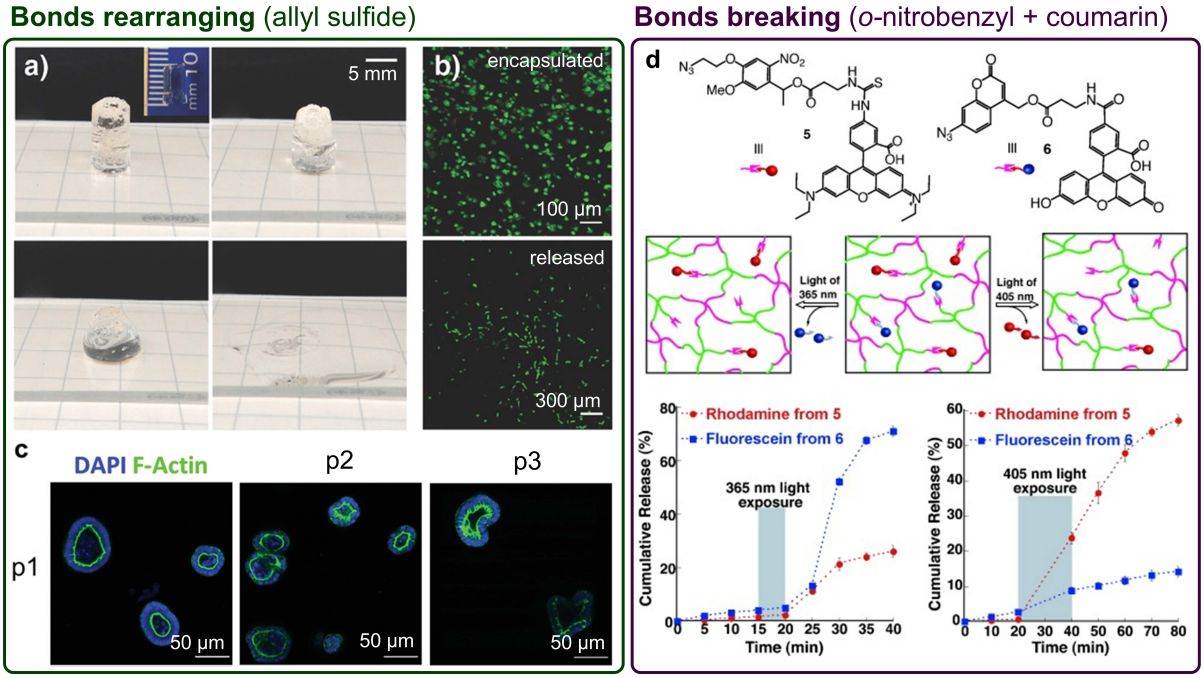

Figure 2. Photodegradation: cell harvesting to release biomolecules. a) Amplified photodegradation of a hydrogel with AlS crosslinks b) viability of human MSCs before and after AlS photodegradation (adapted with permission from ref. (26), Copywrite 2017 Wiley-VCH). c) Murine intestinal organoids passaged using photodegradable AlS hydrogels through passage 3 (adapted with permission from ref. (31), Copywrite 2020 Wiley-VCH) d) Sequential release of rhodamine (red) and fluoresceine (blue) using the excitation wavelengths 405 nm for *o*-Nb and 365 nm for coumarin methyl ester photolysis (adapted with permission from ref. (36), Copywrite 2013 Wiley-VCH).

3.1.3. Intracellular gelation to induce and reverse cell stasis via photodegradable linkers (o-Nb)

Animals such as tardigrades can enter a state of reversible protective stasis to endure extreme conditions.[37] Such a process could be beneficial for storage of blood and cell products or protecting organs before transplantation. We were interested in if molecular crowding via reversible intracellular polymer assembly could achieve similar effects. To that end, we developed methods to deliver and assemble hydrogel networks intracellularly to slow cellular activity and then reverse the stasis on demand. Specifically, *o*-Nb-containing DBCO- and azide-functionalized macromers were sequentially transfected into a breast cancer cell line (MCSF10As), both as single cells[38] and spheroids[39] (Figure 3a), and intracellular gelation led to slowed cell cycle progression, as well as decreased metabolic activity and protein synthesis. Then, upon network disassembly via photodegradation of the *o*-Nb linker with 365 nm irradiation, cellular activities recovered, including proliferation, metabolic activity, protein translation, and motility (Figure 3b).[38] Towards a more complex tissue model, the process was tested on MCF10A tumor spheroids, where transfection could be performed in 3D to induce a

quiescent cell population and reduce bioenergetics and metabolic rates. When the *o*-Nb moieties were photodegraded, biostasis was reversed, and spheroid proliferation returned to normal activity levels.[39] In general, these innovative methods suggest the possibilities of reversible biostasis for storage and transport of cell and tissue products to remote locations.

3.1.4. Photo-responsive materials for high resolution imaging in 3D: Expansion microscopy (AlS)

Matrices used for 3D culture of cells, multicellular constructs, and dense tissues can complicate high resolution imaging due to light scattering and absorption. In addition, many super resolution imaging methods are not compatible with 3D samples. To overcome some limitations of optically imaging these constructs, Boyden *et al.*, exploited responsive polyelectrolyte hydrogels to develop expansion microscopy.[40,41] Building from these ideas, our group recently developed a protocol for photo-expansion microscopy that is compatible with cell-laden gels and can be repeated multiple times (Phototransfer by Allyl Sulfide-Exchange Expansion Microscopy, PhASE-ExM).[1] The method enables optical clearance and super resolution imaging of thick tissues and cell-laden hydrogel samples, and its applicability was demonstrated with large intestinal organoids. PhASE-ExM combines two previous technologies developed in this lab: 1) AlS photo-responsive hydrogels used for intestinal organoid culture[26,31] (section 3.1.1) and 2) a photopolymerized expansion hydrogel that uses a thiol-acrylate mix-mode polymerization to create a highly swellable, polyelectrolyte network (PhotoExM, Figure 3c).[42] In PhASE-ExM, photodegradation and AlS exchange between the original network and expansion network results in a gel-to-gel transfer of alkene functionalized antibodies.[1] The PhASE-ExM formulation can achieve 4.6 - 6.7x hydrogel expansion[42] (Figure 3d) facilitating <120 nm resolution to image deposited collagen IV and integrin β1 interactions in intestinal organoid crypts (Figure 3e).[1] PhotoExM and PhASE-ExM facilitate investigations of difficult to image cell-cell and cell-materials interactions at the sub-micron size scale in 3D.

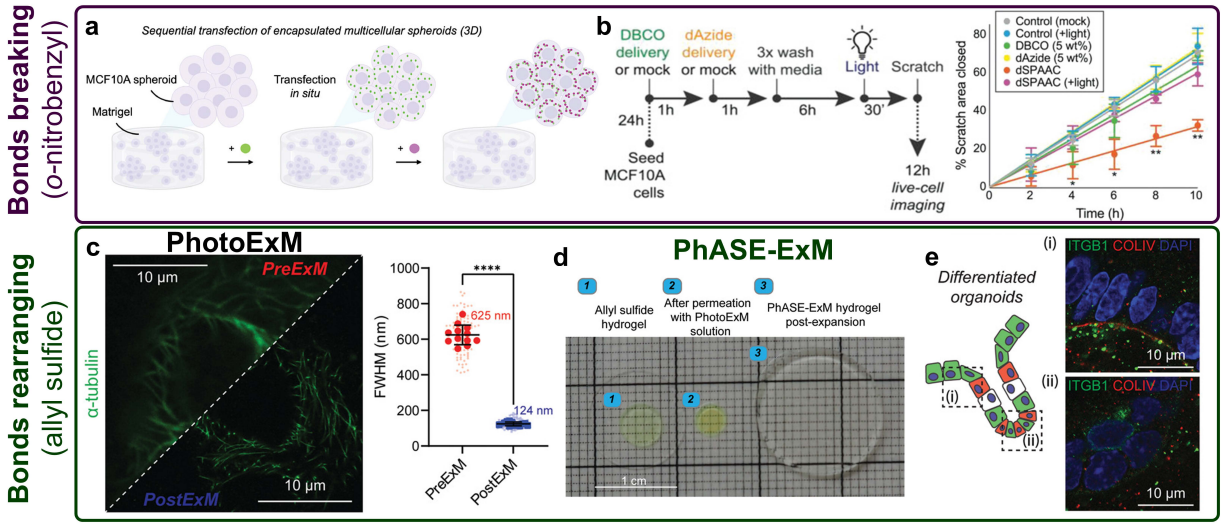

Figure 3. Photodegradation: applications in biostasis and imaging. a) Illustration of how the photodegradable SPAAC network is transfected within cells to slow intracellular processes. (adapted with permission from ref. (39), Copywrite 2023 Wiley-VCH). b) Timeline of biostasis transfection showing reduced cell migration with SPAAC treatment (orange) and recovered cell proliferation and migration following light exposure to degrade the *o*-Nb moieties and reverse intracellular gelation (pink). (adapted with permission from ref. (38), Copywrite 2022 Wiley-VCH). c) α-tubulin imaging pre- and post-expansion demonstrating the improvement in resolution using the full width half max (FWHM) of microtubule diameter (**** p<0.0001). d) Visual depiction of hydrogel swelling after fluorophore transfer. e) PhASE-ExM images showing the organization of integrin β1 and collagen IV within the (i) hinge and (ii) crypt regions of the organoid post-differentiation. (adapted with permission from ref. (1), Copywrite 2022 Wiley-VCH).

3.2. Photodegradation – Partial Network Bond Breaking for Controlled Mechanical Properties

As opposed to complete network erosion, partial degradation of network crosslinks allows for controlled manipulation of material properties, including modulus, diffusivity, and swelling. When the hydrogel crosslinks are cleaved in the presence of cells, the dynamics of mechanosensing and cell-cell signaling can be studied.

3.2.1. Network softening in 2D cell cultures – recovery of regenerative potential (o-Nb, AlS)

When MSCs are expanded *ex vivo*, the substrate used can influence the proliferation, secretory properties and multipotency of stem cells, changing their therapeutic potential *in vivo*.[43] MSCs are widely studied and used in clinical trials, so our group and others have extensively studied methods to mitigate and reverse the loss of the regenerative and therapeutic potential of MSCs. We have demonstrated that transferring MSCs from physiologically stiff tissue culture plasticware (~1 GPa) to soft hydrogel substrates can revive the regenerative phenotype, increasing proliferation rates, stem marker expression, and secretory profiles.[44–46] A follow-up study with AlS photo-softening hydrogels confirmed that this change was related to epigenetic changes in the nucleus (*e.g.,* histone acetylation and chromatin condensation), inducing a mechanical memory in the hMSCs (Figure 4a).[2] Collectively, this work led to the identification of HAT1 and HDAC1, 2, and 3 as key determinants of the (ir)reversibility of histone acetylation.[2] Beyond MSCs, using *o*-Nb-mediated photo-softening, similar changes

were observed with valvular interstitial cells (VICs), where nuclear mechanosensing and chromatin signatures played an equally important role in the induction of fibroblasts to persistently activated myofibroblasts that are observed in fibrotic heart valves.[47]

3.2.2. Network softening in 3D – studying and controlling intestinal organoid crypt formation (AlS)

Beyond individual cells sensing matrix mechanics, sheets of epithelial cells can respond to matrix softening by buckling and altering local curvature.[48] In this way, temporally controlled degradation of hydrogels have been exploited to induce crypt formation during the differentiation of intestinal organoids.[49] Specifically, AlS hydrogels were used to systematically control the crosslinking density in intestinal organoid-laden hydrogels by precise increments, based on the duration of light exposure (0, 2, 5, 8 and 10 seconds) in the presence of glutathione and LAP. Through this experimental design, an initially stiff matrix that supported colony formation could be softened over a range of matrix moduli to discover conditions that support organoid differentiation (Figure 4b, ii).[49] In brief, if the matrix modulus change was modest (0, 2 sec), organoid differentiation and crypt formation was limited, and if the matrix was softened too much, the crypt forming efficiency was also negatively impacted. An intermediate decrease in crosslinking density (5 sec of photodegradation) was the most advantageous for crypt formation, implicating an important role of mechanosensing in not only crypt formation (Figure 4b, iii), but crypt length and the number of crypts per colony (Figure 4b, vi-v).

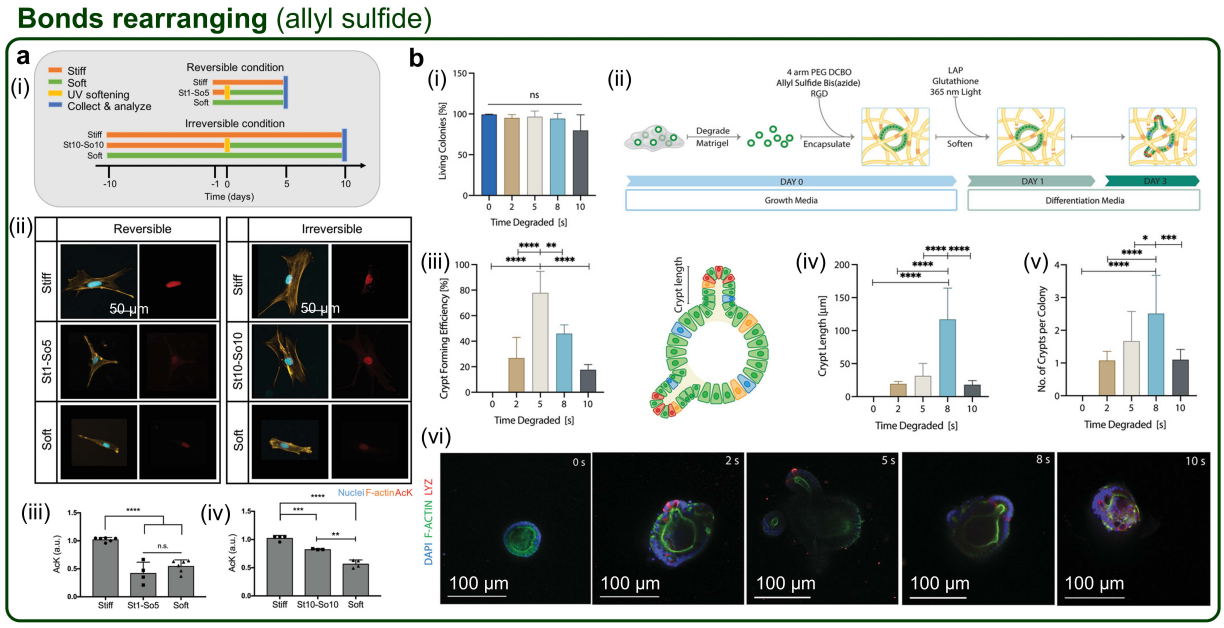

Figure 4. Photo-softening: recovery of stemness and organoid crypt formation. a) (i) Timeline of *in situ* photo-softening for the reversible and irreversible histone acetylation. (ii) Fluorescence images showing the reversible and irreversible nuclear localization of AcK on the left and right, respectively. Quantification of AcK intensity in (iii) reversible and (iv) irreversible conditions. (adapted with permission from ref. (2), Copywrite 2018 Wiley-VCH). b) (i) Organoids remained viable under 10 seconds of light irradiation. (ii) Schematic detailing the encapsulation, growth, photo-softening, and differentiation timeline for intestinal organoids within AlS hydrogels. Quantification of (iii) crypt forming efficiency, (iv) crypt length, and (v) number of crypts per colony to identify the optimal time of light irradiation for organoid differentiation with corresponding (vi) fluorescence images. (adapted with permission from ref. (50), Copywrite 2020 Wiley-VCH).

3.3. Photo-stiffening – In situ Bond Formation

As a corollary to photolysis of network bonds, the *in situ* formation of crosslinks and resultant matrix stiffening are relevant to many biological processes, as many tissues become stiffer with disease and aging.

3.3.1 Photo-stiffening while supporting cell spreading and matrix interactions: applications to cardiac cells (anthracene dimerization and strained alkyne photo-oligomerization)

Many tissue-resident fibroblasts (*e.g.,* skin, lung, heart, kidney liver) are responsible for wound repair and tissue homeostasis; fibroblasts activate to a myofibroblast phenotype with elevated migration, secretory properties and contractility. Upon resolution of the injury, the quiescent fibroblast phenotype typically returns, but if the myofibroblast phenotype persists, excess ECM is deposited, and fibrotic disease or scarring can occur. The effect is exaggerated by changes in tissue stiffness. However, less is known about the fate of the myofibroblast and to date, few drugs exist for reversing the effects of fibrotic disease. Towards the goal of identifying new treatments, Günay *et al.* developed a PEG-anthracene macromer that allowed us to temporally control the hydrogel modulus via light without the addition of exogenous molecules and in complex cell media (Figure 5a-b).[21] Using cardiac

fibroblasts, we demonstrated that matrix stiffening (10 – 50 kPa) influenced the activation of nuclear factor of activated T cells (NFAT), which translocated into the nucleus, demonstrating rapid calcium transience (within 6 minutes) after the cardiac fibroblast were subjected to an increase in microenvironment modulus (Figure 5c-d).[21] This system has great potential to be translated to study VICs in the context of aortic valve stenosis[47,51–53] and used for 3D culture[54] in the future.

3.3.2 Photo-stiffening influences cell proliferation and motility: applications in muscle aging and regeneration (strained alkyne photo-oligomerization)

In this next application, we built upon and found utility for a unique phenomenon observed with SPAAC crosslinked networks. Brown *et al.* observed that if SPAAC networks with 2 or 3 equivalents of excess strained alkyne were exposed to light in the presence of a photoinitator, the hydrogel storage modulus increased 230% or 680% the initial values, respectively (Figure 5e).[20] Silver *et al.* then exploited this secondary DBCO photo-oligomerization to create synthetic ECM microenvironments with moduli that mimicked and spanned the changes observed in muscle tissue after injury. By increasing the modulus of the uninjured muscle niche *in situ*, results revealed that muscle stem cells (MuSCs) became activated and began proliferating mimicking the cellular responses that occur during muscle regeneration. However, after a major muscle injury *in vivo*, healing results in a persistent, stiff, fibrotic ECM, which prevents MuSC return to a quiescent state and alters the regenerative capacity during subsequent injuries. However, inhibition of mechanosensing via knockout of both yes-associated protein 1 (YAP) and its orthogonal transcriptional coactivator with a PDZ-binding domain (TAZ) can restore MuSC quiescence (Figure 5f-g).[3,55]

3.3.3 Photo-stiffening alters nuclear mechanosensing: mechanisms of outside-in signaling and epigenetic changes (strained alkyne photo-oligomerization)

MSCs respond to photo-softening of their microenvironment by decreases in cell area, reduction in cytoskeletal tension, and redistribution of YAP out of the nucleus and into the cytoplasm. However, foundational studies further that when the microenvironment is stiffened using secondary photo-crosslinking reactions, MSC spreading increases, actin cytoskeletal tension increases, and YAP translocates back into the nucleus.[45] Specifically, using the DBCO photo-oligomerization system, Killaars *et al.* identified that MSC nuclear tension, characterized by Lamin A intensity, increased significantly during the 3-6 days following photo-stiffening (Figure 5h-j). Further, this caused an increase in nuclear tension, and subsequent chromatin and epigenetic remodeling, as observed by changes in global histone acetylation. Of note, these finding complement observations with MSCs and valve fibroblasts, which undergo (ir)reversible histone acetylation after photo-softening, depending on the "mechanical dose" or time in stiff microenvironments (section 3.2.1).[2,47] Photo-stiffening was correlated with

markers of osteogenesis in MSCs, and the findings were linked to dysregulation of osteogenic differentiation due to histone-deacetylation in MSC phenotypes associated with bone degenerative diseases.[56]

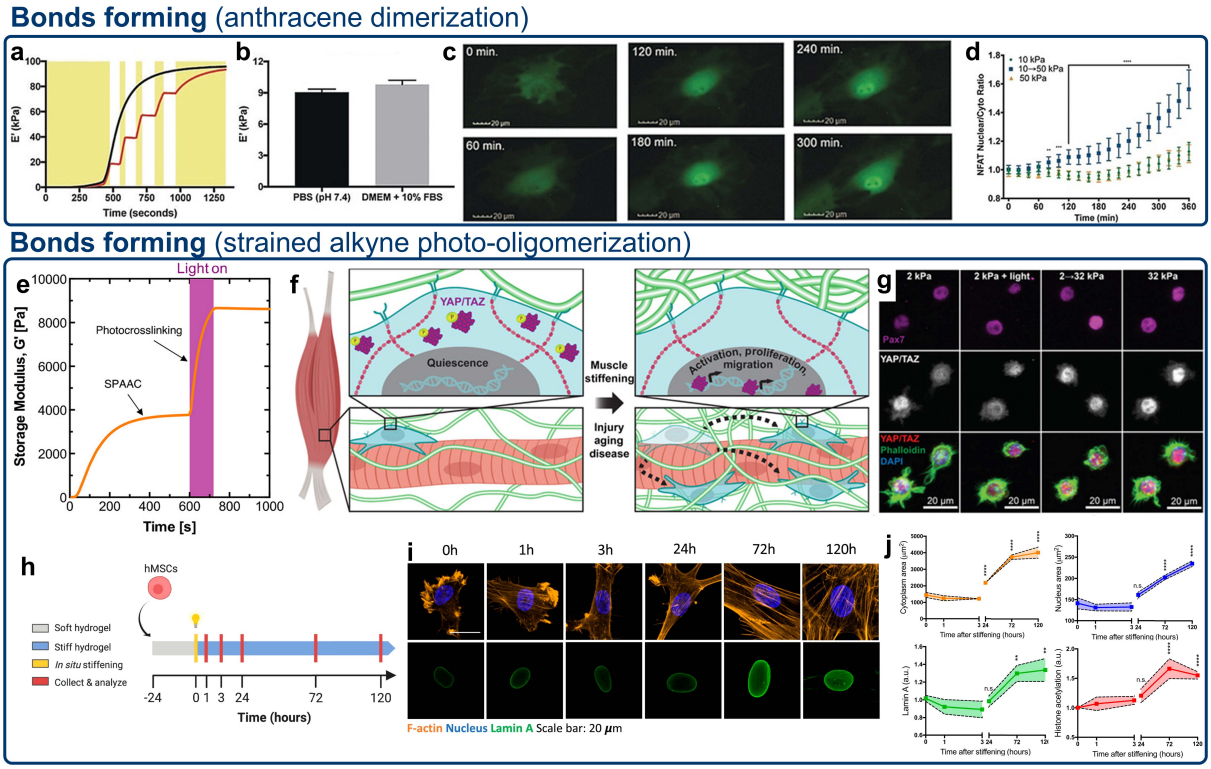

Figure 5. Photo-stiffening: from investigating mechanobiology to modeling diseased tissues. a) *In situ* gelation of the PEG-anthracene hydrogel with continuous light (black) or pulsed light (red). b) Comparison of modulus after gelation in PBS vs. DMEM + 10% FBS. c) Fluorescence images showing the nuclear translocation of NFAT over 300 minutes and d) quantification of the nuclear/cytoplasmic ratio of NFAT under static or transient stiffening (blue, square) (adapted with permission from ref. (21), Copywrite 2019 Wiley-VCH). e) Photo-stiffening post-network formation via DBCO photo-oligomerization under light irradiation (adapted with permission from ref. (20), Copywrite 2018 American Chemical Society). f) Illustration demonstrating how the nuclear translocation of YAP/TAZ is indicative of injury, aging, and disease in muscle cells. g) Fluorescence images depicting the nuclear translocation of YAP/TAZ (grey) after substrate stiffening (2 → 32 kPa). (adapted with permission from ref. (3), Copywrite 2021 Wiley-VCH) h) Timeline of experiment to test the effect of *in situ* stiffening. i) Fluorescence images showing the increasing intensity of Lamin A in the nucleus with time after network stiffening. j) Quantification of the cytoplasmic area (yellow), nucleus area (blue), Lamin A intensity (green) and histone acetylation intensity (red) with time after stiffening. (adapted with permission from ref. (56), Copywrite 2020 National Academy of Sciences).

3.4 Photo-patterning – Precision Network Modifications Through Spatially Controlled Reactions

The ECM is a dynamic environment defined by transient biochemical and biomechanical signals. Spatiotemporal precision photo-patterning of hydrogels allows one to recapitulate aspects of these variations, in a user-defined manner to control both cell-matrix interactions and cell-cell signaling.[5,57,58,7,59]

3.4.1 Patterned and templated 2D surfaces for cell culture and recovery (o-Nb, dithiolane)

Photomasks can be used to precisely control light illumination and initiate photo-cleavage reactions or network erosion along the x and y planes of a hydrogel.[26,60–63] In one example, Magin *et al.* degraded hydrogels using *o*-Nb photolysis through 2μm x 2μm tiled photomasks (mimicking the size of cellular focal adhesions) to yield substrates that were 0, 11, 25, 75, and 100% stiff by area (Figure 6a-b).[61] When either MSCs[60] or VICs[62,63] were seeded on top of these patterned matrices, cells responded by forming focal adhesions and translocating YAP into the nucleus due to cellular mechanotransduciton (Figure 6c,i-ii and 6d). Further, these outside-in spatially defined signals promoted osteogenic differentiation of MSCs and myofibroblast activation of valve fibroblasts, in a manner that depended on the dose of stiff regions. However, when the regular patterned stiff regions were randomized, cellular focal adhesions decreased and YAP nuclear localization was diminished indicating reduced cellular mechanosensing (Figure 6c,iii and 6d).[60] Therefore, precision patterning can elucidate how cells respond to nuanced changes in ECM organization.

Photopatterning has also been used to sequentially present, remove, and exchange biomolecules (e.g., peptide, protein) using bond rearrangement chemistries. In one example, Grim *et al.* used AlS moieties to reversibly pattern cytokines in both 2D (using photomasks) and 3D (using a two-photon laser scanning confocal microscope)[24] (Figure 6e). Valve fibroblasts responded to local concentrations of TGF-β1, activating to myofibroblasts, demonstrating bioactivity of the protein and the ability to spatially control cellular responses.[24] In recent complementary work, other bond rearrangement techniques have been explored (*e.g.,* 1,2-dithiolane reversible ROP), which were used to selectively pattern the presentation of the fibronectin-derived cell adhesive ligand, RGD. Circular islands of RGD were able to direct NIH 3T3s and C2C12s interactions and adhesion (Figure 6f).[29] In addition, subsequent photochemical reactions were used to remove the RGD, release and capture cells from defined regions.[18,29,64] Spatiotemporal control of matrix adhesivity have beneficial in applications, such as microdevices designed to capture rare cell types from complex solutions (*e.g.,* circulating tumor cells), and then subsequently release them for analysis and testing.[65,66]

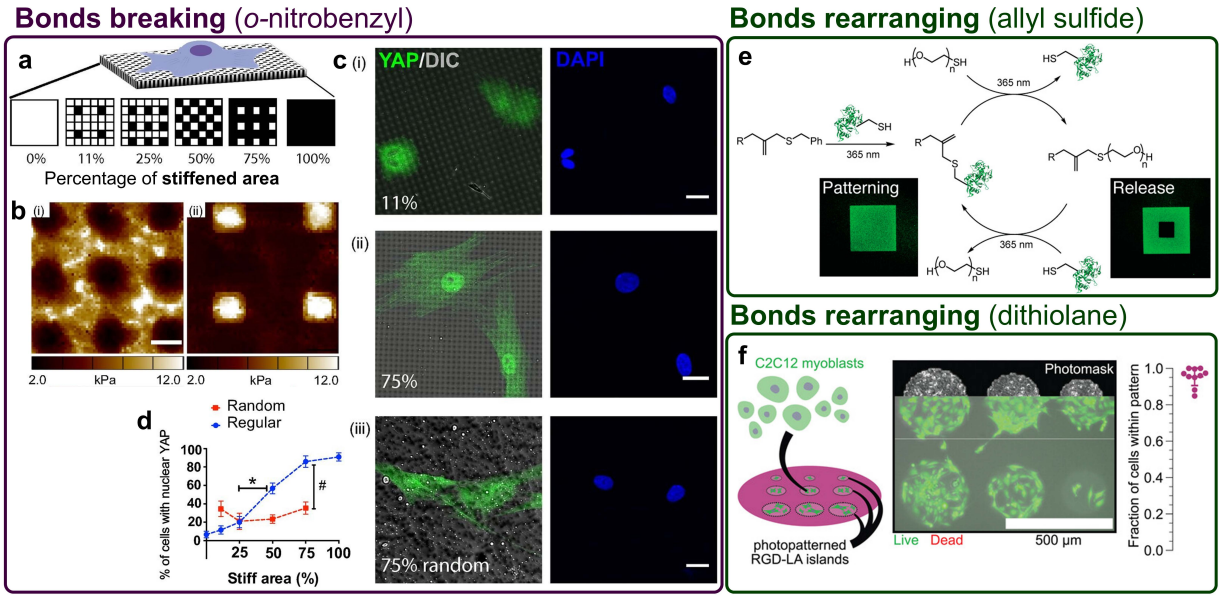

Figure 6. 2D Precision patterning to control cell-substrate interactions. a) Photodegraded surfaces with different percentages of stiff area. b) Atomic force microscopy images of the (i) 75% and (ii) 11% stiff conditions. c) Fluorescent and differential interference contrast (DIC) images showing the nuclear translocation of YAP across the (i) 11% stiff, regular, (ii) 75% stiff, regular, and (iii) 75% stiff, random substrates. d) Percentage of cells with nuclear YAP across increasing total stiff areas between regular (blue) and randomly (red) patterned substrates. (adapted with permission from ref. (60), Copywrite 2016 National Academy of Science). e) Circular patterning and release cycle of biomolecules using AlS exchange reactions (adapted with permission from ref. (24), Copywrite 2018 American Chemical Society). f) Photopatterned regions of lipoic acid functionalized RGD (RGD-LA) to spatially pattern the adherence of C2C12 myoblasts (adapted with permission from ref. (29), Copywrite 2023 Wiley-VCH).

3.4.2 Patterning physiologically relevant microstructures in 3D (o-Nb)

Beyond photomasks and creation of 2D patterns (x and y) on cell-seeded hydrogel systems, single and two-photon laser scanning confocal microscopy allows precise formation of complex structures (*e.g.,* wells, channels, arbitrary shapes), in 3D (x, y, and z).[18,67] Using these photopatterning methods, much of our work has relied on *o*-Nb-containing hydrogels. For example, towards the development of an *in vitro* model of the lung epithelium, *o*-Nb-containing photodegradable microspheres were fabricated and used to generate spherical cystic structures of lung alveoli with hollow cores (Figure 7a-b).[68,69] Precision erosion methods were used to pattern wells of varying dimensions and connectivity to understand the influence of alveoli curvature on lung AT-2 progenitor cell location (Figure 7c-d).[70] In another example, neurospheres (composed of embryonic stem-cell derived motor neurons) were cultured in wells, and channels of different sizes were eroded proximal to the neurosphere to study the effects of contact guidance on motor axon extension in three-dimensions[71] (Figure 7e-f) and intestinal organoid crypt morphogenesis, *vide infra*.

3.4.3 Precise photo-patterning to direct crypt formation in intestinal organoids (o-Nb and AlS)

Intestinal organoids can be grown from single ISCs and will self-assemble and differentiate to recapitulate the cells and structures found in the parent organ.[49] We sought to direct organoid formation in a predictable manner by utilizing photo-patternable hydrogels to direct intestinal organoid growth and differentiation into those with uniform shapes and sizes. In our initial work, intestinal stem colonies were embedded in *o*-NB hydrogels matrices and two-photon irradiation was used to photodegrade the network in distinct channels with crypt like dimension adjacent to the colony.[48] Immediately after patterning, the organoid epithelium deforms into the patterned space, altering tension, mechanosensing, and ultimately changes in YAP/TAZ signaling (Figure 7g, i-v).[4,48] When combined with the timing of transitioning the culture to differentiation media (4D), crypts form exclusively in the photopatterned regions and are absent from regions that are unmodified (Figure 7g,vi).[48]

As an alternative method to direct crypt formation, we utilized photo-induced AlS exchange to relieve the local stress generated by intestinal organoid colony growth within the elastic confinement of a 3D hydrogel scaffold. When irradiated with light in the presence of a soluble photoinitiator, network tethered thiyl radicals are generated, propagating and creating consequent exchange reactions that lead to bond rearrangement, thus relaxing local stresses surrounding the growing organoid (Figure 7h).[4] Network rearrangements only occur in illuminated regions, and the organoids sense the patterned stress-relaxation and locally deform (Figure 7i). When the organoids were subsequently exposed to differentiation conditions and bulk photo-softened, differentiated crypts were more likely to form in areas of induced viscoelasticity.[4] This indicates that by alleviating the local stress distribution in defined regions we can prime organoid for crypt formation via cell-shape (epithelial curvature) induced mechanotransduction.

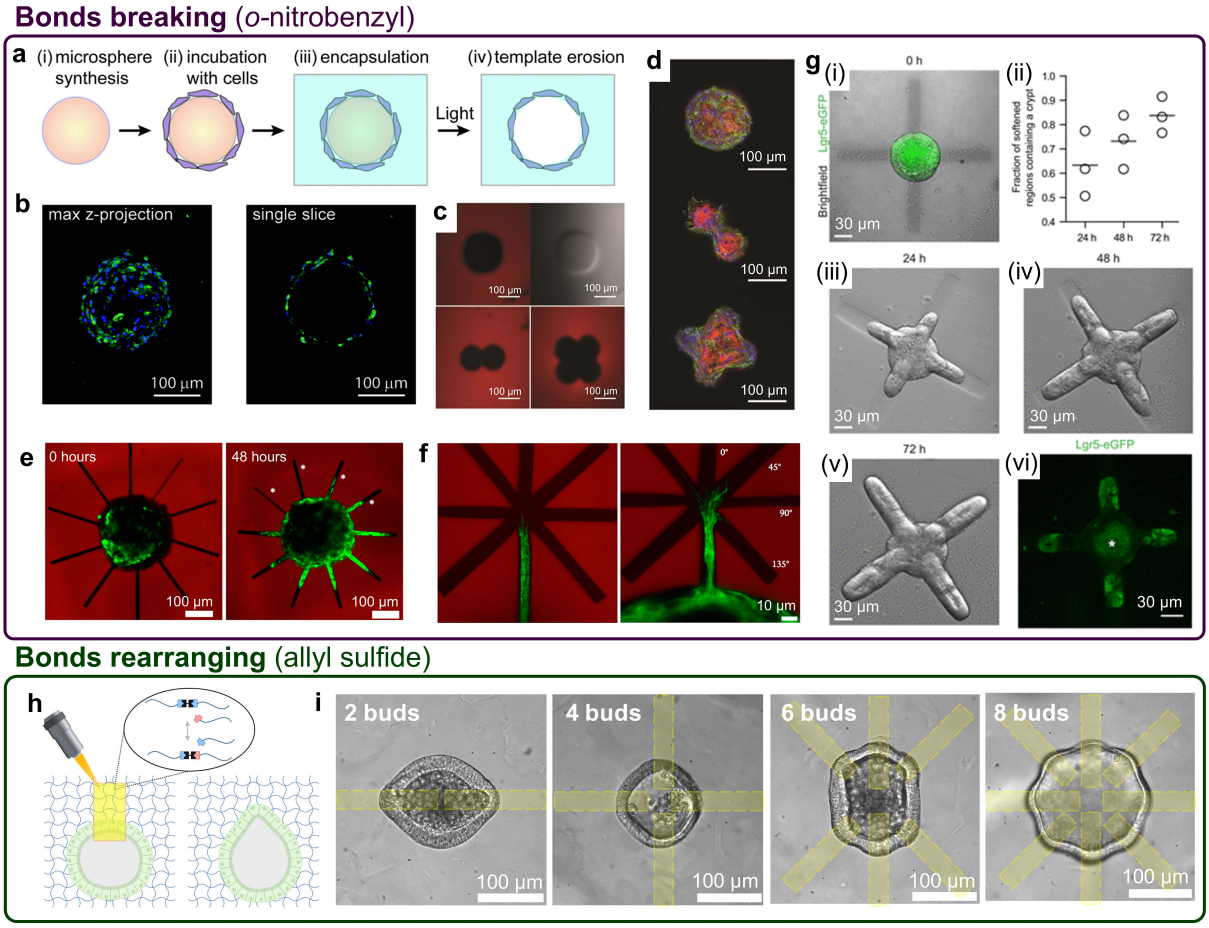

Figure 7. Photo-patterning to enable morphogenesis of multicellular constructs. a) Illustration of lung alveoli patterning process around microspheres, encapsulation, and subsequent photodegradation. b) Fluoresces images of a templated lung alveoli and a cross-section showing the hollow core. (adapted with permission from ref. (69), Copywrite 2015 Royal Society of Chemistry). c) Photopatterned wells for lung alveoli with 1, 2, and 4 lobes. d) Successful culture of lung alveoli within the patterned wells (adapted with permission from ref. (70), Copywrite 2014 Oxford University Press). e) Encapsulated neurosphere with eroded channels immediately and 48 hours after patterning. Channels marked with an asterisk were not completely eroded. f) Fork-shaped patterns before (left) and after (right) the axons reached the fork showing preferred directionality at 45°. (adapted with permission from ref. (71), Copywrite 2014 American Chemical Society). g) (i) photodegraded cross structure around a spherical intestinal organoid (green, stem cells, Lgr5+). (ii) Quantification of the percentage of patterned region that is filled by the organoid over (iii) 24, (iv) 48, and (v) 72 hours after patterning. (vi) Fluorescence image showing the migration of Lgr5+ stem cells to the ends of the patterned crypts. Asterisk denotes autofluorescence of the dead cells shed into the organoid core (adapted with permission from ref. (48), Copywrite 2022 AAAS). h) Illustration light induced viscoelasticity to pattern regions around an encapsulated intestinal colony. i) Brightfield images of patterned organoids deforming into the patterned regions with 2-8 buds after patterning. (adapted with permission from ref. (4), Copywrite 2023 AAAS).

IV. Summary and Future Outlook

The work presented here demonstrates the utility of light as a stimulus to guide cellular processes and as a tool to manipulate microenvironments with user-control. The contributions of Anseth and coworkers, highlighted above, demonstrate how a "toolbox" of photoactivated network bond-breaking, -forming, and -

rearranging reactions can be applied creatively to change the mechanical properties and functionality of hydrogels in the presence of cells to answer in-depth biological questions. We have demonstrated the utility of network degradation to recover encapsulated cells, deliver biological factors during culture, reverse molecular biostasis, and improve the resolution of fluorescence imaging techniques. In addition, partial photodegradation facilitated the study of stem cells, valve fibroblasts, and intestinal organoids in the context of differentiation and regenerative potential. Network photo-stiffening has been used to model diseased tissue niches and elucidate the biochemical pathways that contribute to disease progression and possible therapeutic treatments. Finally, single and multi-photon photopatterning was used to template surfaces on biologically relevant length scales, guide cellular morphogenesis, and in particular, make strides in improving the stochastic organization of multicellular constructs over those observed in biologically derived culture matrices.

Bio-orthogonal, synthetic hydrogels engineered to contain light-activated moieties enable user-control over the cellular microenvironment in the presence of otherwise biochemically complex systems. The limit to how the chemical toolbox described in this Account can be used is defined only by the creativity of the user. We envision great strides being made in the fields of biomaterials and tissue engineering as these tools are continually applied to the following spaces: 1) photo-activated control over network viscoelastic and nonlinear elastic properties, 2) improvements in cycling between soft and stiff microenvironments, 3) the implementation of digital light processing to fabricate hierarchical cellular and tissue constructs, 4) incorporation of photo-actuators to enable hydrogel shape changes, 5) refinement of temporal and spatial resolution during photopatterning to achieve physiologically accurate tissue constructs, and 6) the continued implementation of photo-labile moieties and application of state-of-the-art detectors to image cell-matrix interactions and cellular processes in real-time. The development of the next generation of photoactive hydrogels will require the discovery of new network modulating chemistries and/or the interdisciplinary integration of existing moieties from other spaces. The continued implementation and innovation of such materials will accelerate the field towards its ultimate goal of clinical actualization.

V. Authors' Biosketches

Ella A. Hushka earned her B.S. with honors in Chemical and Biological Engineering from the University of Colorado Boulder in 2018. She is currently a Ph.D. candidate in the department of Chemical and Biological Engineering at the University of Colorado Boulder as an NSF Graduate Research Fellow under the advisement of Prof. Kristi S. Anseth.

Monica L. Ohnsorg obtained her (ACS certified) B.S. in Chemistry with minors in Engineering and Mathematics from Hope College in 2016. As an NSF Graduate Research Fellow, she received her Ph.D. in Chemistry from the University of Minnesota co-advised by Prof. Theresa M. Reineke and Prof. Frank S. Bates. Currently, she is a postdoctoral fellow in the lab of Prof. Kristi S. Anseth at the University of Colorado Boulder.

Kristi S. Anseth is a Distinguished Professor, Tisone Professor of Chemical Engineering, and Associate Director of the BioFrontiers Institute at the University of Colorado Boulder. She is also an elected member of the US National Academy of Engineering, National Academy of Medicine, National Academy of Sciences, and National Academy of Inventors.

Acknowledgements: The authors are grateful for the many students, postdoctoral researchers, collaborators, and staff without whom the research described here would not have been possible. The work described above was supported by the National Institutes of Health (R01 DE016523, R01 DK120921, and R01 HL132353), National Science Foundation (DMR 1006711 and RECODE 2033723), Howard Hughs Medical Institute, and Defense Advanced Research Projects Agency (W911NF-19–2-0024). The authors were additionally supported by National Institutes of Health T32 AR080630 (M. L. O.) and National Science Foundation Graduate Research Fellowship Program DGE 2040434 (E. A. H.).

References:

(1) Blatchley, M. R.; Günay, K. A.; Yavitt, F. M.; Hawat, E. M.; Dempsey, P. J.; Anseth, K. S. In Situ Super-Resolution Imaging of Organoids and Extracellular Matrix Interactions via Phototransfer by Allyl Sulfide Exchange-Expansion Microscopy (PhASE-ExM). *Adv. Mater.* **2022**, *34* (16), 2109252. https://doi.org/10.1002/adma.202109252.

(2) Killaars, A. R.; Grim, J. C.; Walker, C. J.; Hushka, E. A.; Brown, T. E.; Anseth, K. S. Extended Exposure to Stiff Microenvironments Leads to Persistent Chromatin Remodeling in Human Mesenchymal Stem Cells. *Adv. Sci.* **2019**, *6* (3), 1801483. https://doi.org/10.1002/advs.201801483.

(3) Silver, J. S.; Günay, K. A.; Cutler, A. A.; Vogler, T. O.; Brown, T. E.; Pawlikowski, B. T.; Bednarski, O. J.; Bannister, K. L.; Rogowski, C. J.; Mckay, A. G.; DelRio, F. W.; Olwin, B. B.; Anseth, K. S. Injury-Mediated Stiffening Persistently Activates Muscle Stem Cells through YAP and TAZ Mechanotransduction. *Sci. Adv.* **2021**, *7* (11), eabe4501. https://doi.org/10.1126/sciadv.abe4501.

(4) Yavitt, F. M.; Kirkpatrick, B. E.; Blatchley, M. R.; Speckl, K. F.; Mohagheghian, E.; Moldovan, R.; Wang, N.; Dempsey, P. J.; Anseth, K. S. In Situ Modulation of Intestinal Organoid Epithelial Curvature through Photoinduced Viscoelasticity Directs Crypt Morphogenesis. *Sci. Adv.* **2023**, *9* (3), eadd5668. https://doi.org/10.1126/sciadv.add5668.

(5) Brown, T. E.; Anseth, K. S. Spatiotemporal Hydrogel Biomaterials for Regenerative Medicine. *Chem. Soc. Rev.* **2017**, *46* (21), 6532–6552. https://doi.org/10.1039/C7CS00445A.

(6) Ruskowitz, E. R.; DeForest, C. A. Photoresponsive Biomaterials for Targeted Drug Delivery and 4D Cell Culture. *Nat. Rev. Mater.* **2018**, *3* (2), 17087. https://doi.org/10.1038/natrevmats.2017.87.

(7) Yavitt, F. M.; Kirkpatrick, B. E.; Blatchley, M. R.; Anseth, K. S. 4D Materials with Photoadaptable Properties Instruct and Enhance Intestinal Organoid Development. *ACS Biomater. Sci. Eng.* **2022**, *8* (11), 4634–4638. https://doi.org/10.1021/acsbiomaterials.1c01450.
(8) Francis, R. M.; DeForest, C. A. 4D Biochemical Photocustomization of Hydrogel Scaffolds for Biomimetic Tissue Engineering. *Acc. Mater. Res.* **2023**, *4* (8), 704–715. https://doi.org/10.1021/accountsmr.3c00062.
(9) Borelli, A. N.; Young, M. W.; Kirkpatrick, B. E.; Jaeschke, M. W.; Mellett, S.; Porter, S.; Blatchley, M. R.; Rao, V. V.; Sridhar, B. V.; Anseth, K. S. Stress Relaxation and Composition of Hydrazone-Crosslinked Hybrid Biopolymer-Synthetic Hydrogels Determine Spreading and Secretory Properties of MSCs. *Adv. Healthc. Mater.* **2022**, *11*, 2200393. https://doi.org/10.1002/adhm.202200393.
(10) Richardson, B. M.; Wilcox, D. G.; Randolph, M. A.; Anseth, K. S. Hydrazone Covalent Adaptable Networks Modulate Extracellular Matrix Deposition for Cartilage Tissue Engineering. *Acta Biomater.* **2019**, *83*, 71–82. https://doi.org/10.1016/j.actbio.2018.11.014.
(11) Hushka, E. A.; Blatchley, M. R.; Macdougall, L. J.; Yavitt, F. M.; Kirkpatrick, B. E.; Bera, K.; Dempsey, P. J.; Anseth, K. S. Fully Synthetic Hydrogels Promote Robust Crypt Formation in Intestinal Organoids. BioRxiv July 10, 2024. https://doi.org/10.1101/2024.07.06.602364.
(12) Ohnsorg, M. L.; Mash, K. M.; Khang, A.; Rao, V. V.; Kirkpatrick, B. E.; Bera, K.; Anseth, K. S. Nonlinear Elastic Bottlebrush Polymer Hydrogels Modulate Actomyosin Mediated Protrusion Formation in Mesenchymal Stromal Cells. *Adv. Mater.* **2024**, 2403198. https://doi.org/10.1002/adma.202403198.
(13) Fairbanks, B. D.; Macdougall, L. J.; Mavila, S.; Sinha, J.; Kirkpatrick, B. E.; Anseth, K. S.; Bowman, C. N. Photoclick Chemistry: A Bright Idea. *Chem. Rev.* **2021**, *121* (12), 6915–6990. https://doi.org/10.1021/acs.chemrev.0c01212.
(14) Chatani, S.; Kloxin, C. J.; Bowman, C. N. The Power of Light in Polymer Science: Photochemical Processes to Manipulate Polymer Formation, Structure, and Properties. *Polym Chem* **2014**, *5* (7), 2187–2201. https://doi.org/10.1039/C3PY01334K.
(15) Kloxin, A. M.; Kasko, A. M.; Salinas, C. N.; Anseth, K. S. Photodegradable Hydrogels for Dynamic Tuning of Physical and Chemical Properties. *Science* **2009**, *324* (5923), 59–63. https://doi.org/10.1126/science.1169494.
(16) Kloxin, A. M.; Tibbitt, M. W.; Anseth, K. S. Synthesis of Photodegradable Hydrogels as Dynamically Tunable Cell Culture Platforms. *Nat. Protoc.* **2010**, *5* (12), 1867–1887. https://doi.org/10.1038/nprot.2010.139.
(17) Tibbitt, M. W.; Kloxin, A. M.; Sawicki, L. A.; Anseth, K. S. Mechanical Properties and Degradation of Chain and Step-Polymerized Photodegradable Hydrogels. *Macromolecules* **2013**, *46* (7), 2785–2792. https://doi.org/10.1021/ma302522x.
(18) DeForest, C. A.; Anseth, K. S. Cytocompatible Click-Based Hydrogels with Dynamically Tunable Properties through Orthogonal Photoconjugation and Photocleavage Reactions. *Nat. Chem.* **2011**, *3* (12), 925–931. https://doi.org/10.1038/nchem.1174.
(19) Azagarsamy, M. A.; McKinnon, D. D.; Alge, D. L.; Anseth, K. S. Coumarin-Based Photodegradable Hydrogel: Design, Synthesis, Gelation, and Degradation Kinetics. *ACS Macro Lett.* **2014**, *3* (6), 515–519. https://doi.org/10.1021/mz500230p.
(20) Brown, T. E.; Silver, J. S.; Worrell, B. T.; Marozas, I. A.; Yavitt, F. M.; Günay, K. A.; Bowman, C. N.; Anseth, K. S. Secondary Photocrosslinking of Click Hydrogels To Probe Myoblast Mechanotransduction in Three Dimensions. *J. Am. Chem. Soc.* **2018**, *140* (37), 11585–11588. https://doi.org/10.1021/jacs.8b07551.
(21) Günay, K. A.; Ceccato, T. L.; Silver, J. S.; Bannister, K. L.; Bednarski, O. J.; Leinwand, L. A.; Anseth, K. S. PEG–Anthracene Hydrogels as an On-Demand Stiffening Matrix To Study Mechanobiology. *Angew. Chem. Int. Ed.* **2019**, *58* (29), 9912–9916. https://doi.org/10.1002/anie.201901989.
(22) Perrier, S. *50th Anniversary Perspective* : RAFT Polymerization—A User Guide. *Macromolecules* **2017**, *50* (19), 7433–7447. https://doi.org/10.1021/acs.macromol.7b00767.
(23) Gandavarapu, N. R.; Azagarsamy, M. A.; Anseth, K. S. Photo-Click Living Strategy for Controlled, Reversible Exchange of Biochemical Ligands. *Adv. Mater.* **2014**, *26* (16), 2521–2526. https://doi.org/10.1002/adma.201304847.

(24) Grim, J. C.; Brown, T. E.; Aguado, B. A.; Chapnick, D. A.; Viert, A. L.; Liu, X.; Anseth, K. S. A Reversible and Repeatable Thiol–Ene Bioconjugation for Dynamic Patterning of Signaling Proteins in Hydrogels. *ACS Cent. Sci.* **2018**, *4* (7), 909–916. https://doi.org/10.1021/acscentsci.8b00325.

(25) Marozas, I. A.; Cooper-White, J. J.; Anseth, K. S. Photo-Induced Viscoelasticity in Cytocompatible Hydrogel Substrates. *New J. Phys.* **2019**, *21* (4), 045004. https://doi.org/10.1088/1367-2630/ab1309.

(26) Brown, T. E.; Marozas, I. A.; Anseth, K. S. Amplified Photodegradation of Cell-Laden Hydrogels via an Addition–Fragmentation Chain Transfer Reaction. *Adv. Mater.* **2017**, *29* (11), 1605001. https://doi.org/10.1002/adma.201605001.

(27) Fairbanks, B. D.; Singh, S. P.; Bowman, C. N.; Anseth, K. S. Photodegradable, Photoadaptable Hydrogels via Radical-Mediated Disulfide Fragmentation Reaction. *Macromolecules* **2011**, *44* (8), 2444–2450. https://doi.org/10.1021/ma200202w.

(28) Albanese, K. R.; Read De Alaniz, J.; Hawker, C. J.; Bates, C. M. From Health Supplement to Versatile Monomer: Radical Ring-Opening Polymerization and Depolymerization of α-Lipoic Acid. *Polymer* **2024**, *304*, 127167. https://doi.org/10.1016/j.polymer.2024.127167.

(29) Nelson, B. R.; Kirkpatrick, B. E.; Miksch, C. E.; Davidson, M. D.; Skillin, N. P.; Hach, G. K.; Khang, A.; Hummel, S. N.; Fairbanks, B. D.; Burdick, J. A.; Bowman, C. N.; Anseth, K. S. Photoinduced Dithiolane Crosslinking for Multiresponsive Dynamic Hydrogels. *Adv. Mater.* **2023**, 2211209. https://doi.org/10.1002/adma.202211209.

(30) Nelson, B. R.; Kirkpatrick, B. E.; Skillin, N. P.; Di Caprio, N.; Lee, J. S.; Hibbard, L. P.; Hach, G. K.; Khang, A.; White, T. J.; Burdick, J. A.; Bowman, C. N.; Anseth, K. S. Facile Physicochemical Reprogramming of PEG-Dithiolane Microgels. *Adv. Healthc. Mater.* **2023**, 2302925. https://doi.org/10.1002/adhm.202302925.

(31) Yavitt, F. M.; Brown, T. E.; Hushka, E. A.; Brown, M. E.; Gjorevski, N.; Dempsey, P. J.; Lutolf, M. P.; Anseth, K. S. The Effect of Thiol Structure on Allyl Sulfide Photodegradable Hydrogels and Their Application as a Degradable Scaffold for Organoid Passaging. *Adv. Mater.* **2020**, *32* (30), 1905366. https://doi.org/10.1002/adma.201905366.

(32) Sato, T.; Vries, R. G.; Snippert, H. J.; Van De Wetering, M.; Barker, N.; Stange, D. E.; Van Es, J. H.; Abo, A.; Kujala, P.; Peters, P. J.; Clevers, H. Single Lgr5 Stem Cells Build Crypt-Villus Structures in Vitro without a Mesenchymal Niche. *Nature* **2009**, *459* (7244), 262–265. https://doi.org/10.1038/nature07935.

(33) Khire, V. S.; Kloxin, A. M.; Couch, C. L.; Anseth, K. S.; Bowman, C. N. Synthesis, Characterization and Cleavage of Linear Polymers Attached to Silica Nanoparticles Formed Using Thiol-acrylate Conjugate Addition Reactions. *J. Polym. Sci. Part Polym. Chem.* **2008**, *46* (20), 6896–6906. https://doi.org/10.1002/pola.22999.

(34) Tibbitt, M. W.; Han, B. W.; Kloxin, A. M.; Anseth, K. S. Student Award for Outstanding Research Winner in the Ph.D. Category for the 9th World Biomaterials Congress, Chengdu, China, June 1–5, 2012: Synthesis and Application of Photodegradable Microspheres for Spatiotemporal Control of Protein Delivery. *J. Biomed. Mater. Res. A* **2012**, *100A* (7), 1647–1654. https://doi.org/10.1002/jbm.a.34107.

(35) Azagarsamy, M. A.; Alge, D. L.; Radhakrishnan, S. J.; Tibbitt, M. W.; Anseth, K. S. Photocontrolled Nanoparticles for On-Demand Release of Proteins. *Biomacromolecules* **2012**, *13* (8), 2219–2224. https://doi.org/10.1021/bm300646q.

(36) Azagarsamy, M. A.; Anseth, K. S. Wavelength-Controlled Photocleavage for the Orthogonal and Sequential Release of Multiple Proteins. *Angew. Chem.* **2013**, *125* (51), 14048–14052. https://doi.org/10.1002/ange.201308174.

(37) Hesgrove, C.; Boothby, T. C. The Biology of Tardigrade Disordered Proteins in Extreme Stress Tolerance. *Cell Commun. Signal.* **2020**, *18* (1), 178. https://doi.org/10.1186/s12964-020-00670-2.

(38) Macdougall, L. J.; Hoffman, T. E.; Kirkpatrick, B. E.; Fairbanks, B. D.; Bowman, C. N.; Spencer, S. L.; Anseth, K. S. Intracellular Crowding by Bio-Orthogonal Hydrogel Formation Induces Reversible Molecular Stasis. *Adv. Mater.* **2022**, *34* (31), 2202882. https://doi.org/10.1002/adma.202202882.

(39) McNally, D. L.; Macdougall, L. J.; Kirkpatrick, B. E.; Maduka, C. V.; Hoffman, T. E.; Fairbanks, B. D.; Bowman, C. N.; Spencer, S. L.; Anseth, K. S. Reversible Intracellular Gelation of MCF10A Cells Enables

Programmable Control Over 3D Spheroid Growth. *Adv. Healthc. Mater.* **2024**, *13* (7), 2302528. https://doi.org/10.1002/adhm.202302528.

(40) Chen, F.; Tillberg, P. W.; Boyden, E. S. Expansion Microscopy. *Science* **2015**, *347* (6221), 543–548. https://doi.org/10.1126/science.1260088.

(41) Wassie, A. T.; Zhao, Y.; Boyden, E. S. Expansion Microscopy: Principles and Uses in Biological Research. *Nat. Methods* **2019**, *16* (1), 33–41. https://doi.org/10.1038/s41592-018-0219-4.

(42) Günay, K. A.; Chang, T.-L.; Skillin, N. P.; Rao, V. V.; Macdougall, L. J.; Cutler, A. A.; Silver, J. S.; Brown, T. E.; Zhang, C.; Yu, C.-C.; Olwin, B. B.; Boyden, E. S.; Anseth, K. S. Photo-Expansion Microscopy Enables Super-Resolution Imaging of Cells Embedded in 3D Hydrogels. *Nat. Mater.* **2023**, *22* (6), 777–785. https://doi.org/10.1038/s41563-023-01558-5.

(43) Wechsler, M. E.; Rao, V. V.; Borelli, A. N.; Anseth, K. S. Engineering the MSC Secretome: A Hydrogel Focused Approach. *Adv. Healthc. Mater.* **2021**, *10* (7), 2001948. https://doi.org/10.1002/adhm.202001948.

(44) Rao, V. V.; Vu, M. K.; Ma, H.; Killaars, A. R.; Anseth, K. S. Rescuing Mesenchymal Stem Cell Regenerative Properties on Hydrogel Substrates Post Serial Expansion. *Bioeng. Transl. Med.* **2019**, *4* (1), 51–60. https://doi.org/10.1002/btm2.10104.

(45) Rosales, A. M.; Vega, S. L.; DelRio, F. W.; Burdick, J. A.; Anseth, K. S. Hydrogels with Reversible Mechanics to Probe Dynamic Cell Microenvironments. *Angew. Chem. Int. Ed.* **2017**, *56* (40), 12132–12136. https://doi.org/10.1002/anie.201705684.

(46) Yang, C.; Tibbitt, M. W.; Basta, L.; Anseth, K. S. Mechanical Memory and Dosing Influence Stem Cell Fate. *Nat. Mater.* **2014**, *13* (6), 645–652. https://doi.org/10.1038/nmat3889.

(47) Walker, C. J.; Crocini, C.; Ramirez, D.; Killaars, A. R.; Grim, J. C.; Aguado, B. A.; Clark, K.; Allen, M. A.; Dowell, R. D.; Leinwand, L. A.; Anseth, K. S. Nuclear Mechanosensing Drives Chromatin Remodeling in Persistently Activated Fibroblasts. *Nat. Biomed. Eng.* **2021**, *5* (12), 1485–1499. https://doi.org/10.1038/s41551-021-00709-w.

(48) Gjorevski, N.; Nikolaev, M.; Brown, T. E.; Mitrofanova, O.; Brandenberg, N.; DelRio, F. W.; Yavitt, F. M.; Liberali, P.; Anseth, K. S.; Lutolf, M. P. Tissue Geometry Drives Deterministic Organoid Patterning. *Science* **2022**, *375* (6576), eaaw9021. https://doi.org/10.1126/science.aaw9021.

(49) Gjorevski, N.; Sachs, N.; Manfrin, A.; Giger, S.; Bragina, M. E.; Ordóñez-Morán, P.; Clevers, H.; Lutolf, M. P. Designer Matrices for Intestinal Stem Cell and Organoid Culture. *Nature* **2016**, *539* (7630), 560–564. https://doi.org/10.1038/nature20168.

(50) Hushka, E. A.; Yavitt, F. M.; Brown, T. E.; Dempsey, P. J.; Anseth, K. S. Relaxation of Extracellular Matrix Forces Directs Crypt Formation and Architecture in Intestinal Organoids. *Adv. Healthc. Mater.* **2020**, *9* (8), 1901214. https://doi.org/10.1002/adhm.201901214.

(51) Mabry, K. M.; Payne, S. Z.; Anseth, K. S. Microarray Analyses to Quantify Advantages of 2D and 3D Hydrogel Culture Systems in Maintaining the Native Valvular Interstitial Cell Phenotype. *Biomaterials* **2016**, *74*, 31–41. https://doi.org/10.1016/j.biomaterials.2015.09.035.

(52) Wang, H.; Tibbitt, M. W.; Langer, S. J.; Leinwand, L. A.; Anseth, K. S. Hydrogels Preserve Native Phenotypes of Valvular Fibroblasts through an Elasticity-Regulated PI3K/AKT Pathway. *Proc. Natl. Acad. Sci.* **2013**, *110* (48), 19336–19341. https://doi.org/10.1073/pnas.1306369110.

(53) Kloxin, A. M.; Benton, J. A.; Anseth, K. S. In Situ Elasticity Modulation with Dynamic Substrates to Direct Cell Phenotype. *Biomaterials* **2010**, *31* (1), 1–8. https://doi.org/10.1016/j.biomaterials.2009.09.025.

(54) Schroeder, M. E.; Batan, D.; Gonzalez Rodriguez, A.; Speckl, K. F.; Peters, D. K.; Kirkpatrick, B. E.; Hach, G. K.; Walker, C. J.; Grim, J. C.; Aguado, B. A.; Weiss, R. M.; Anseth, K. S. Osteopontin Activity Modulates Sex-specific Calcification in Engineered Valve Tissue Mimics. *Bioeng. Transl. Med.* **2022**, *8* (1), e10358. https://doi.org/10.1002/btm2.10358.

(55) Günay, K. A.; Silver, J. S.; Chang, T.-L.; Bednarski, O. J.; Bannister, K. L.; Rogowski, C. J.; Olwin, B. B.; Anseth, K. S. Myoblast Mechanotransduction and Myotube Morphology Is Dependent on BAG3 Regulation of YAP and TAZ. *Biomaterials* **2021**, *277*, 121097. https://doi.org/10.1016/j.biomaterials.2021.121097.

(56) Killaars, A. R.; Walker, C. J.; Anseth, K. S. Nuclear Mechanosensing Controls MSC Osteogenic Potential through HDAC Epigenetic Remodeling. *Proc. Natl. Acad. Sci.* **2020**, *117* (35), 21258–21266. https://doi.org/10.1073/pnas.2006765117.

(57) Magin, C. M.; Alge, D. L.; Anseth, K. S. Bio-Inspired 3D Microenvironments: A New Dimension in Tissue Engineering. *Biomed. Mater.* **2016**, *11* (2), 022001. https://doi.org/10.1088/1748-6041/11/2/022001.

(58) Qazi, T. H.; Blatchley, M. R.; Davidson, M. D.; Yavitt, F. M.; Cooke, M. E.; Anseth, K. S.; Burdick, J. A. Programming Hydrogels to Probe Spatiotemporal Cell Biology. *Cell Stem Cell* **2022**, *29* (5), 678–691. https://doi.org/10.1016/j.stem.2022.03.013.

(59) Blatchley, M. R.; Anseth, K. S. Middle-out Methods for Spatiotemporal Tissue Engineering of Organoids. *Nat. Rev. Bioeng.* **2023**, *1* (5), 329–345. https://doi.org/10.1038/s44222-023-00039-3.

(60) Yang, C.; DelRio, F. W.; Ma, H.; Killaars, A. R.; Basta, L. P.; Kyburz, K. A.; Anseth, K. S. Spatially Patterned Matrix Elasticity Directs Stem Cell Fate. *Proc. Natl. Acad. Sci.* **2016**, *113* (31). https://doi.org/10.1073/pnas.1609731113.

(61) Magin, C. M.; Anseth, K. S. In Situ Control of Cell Substrate Microtopographies Using Photolabile Hydrogels. *Small* **2013**, *9* (4), 578–584. https://doi.org/10.1002/smll.201201841.

(62) Magin, C. M.; Alge, D. L.; Gould, S. T.; Anseth, K. S. Clickable, Photodegradable Hydrogels to Dynamically Modulate Valvular Interstitial Cell Phenotype. *Adv. Healthc. Mater.* **2014**, *3* (5), 649–657. https://doi.org/10.1002/adhm.201300288.

(63) Ma, H.; Killaars, A. R.; DelRio, F. W.; Yang, C.; Anseth, K. S. Myofibroblastic Activation of Valvular Interstitial Cells Is Modulated by Spatial Variations in Matrix Elasticity and Its Organization. *Biomaterials* **2017**, *131*, 131–144. https://doi.org/10.1016/j.biomaterials.2017.03.040.

(64) DeForest, C. A.; Anseth, K. S. Photoreversible Patterning of Biomolecules within Click-Based Hydrogels. *Angew. Chem.* **2012**, *124* (8), 1852–1855. https://doi.org/10.1002/ange.201106463.

(65) LeValley, P. J.; Tibbitt, M. W.; Noren, B.; Kharkar, P.; Kloxin, A. M.; Anseth, K. S.; Toner, M.; Oakey, J. Immunofunctional Photodegradable Poly(Ethylene Glycol) Hydrogel Surfaces for the Capture and Release of Rare Cells. *Colloids Surf. B Biointerfaces* **2019**, *174*, 483–492. https://doi.org/10.1016/j.colsurfb.2018.11.049.

(66) Tibbitt, M. W.; Anseth, K. S.; Kloxin, A. M.; Toner, M.; Oakey, J.; Shah, A. SELECTIVE CAPTURE AND RELEASE OF RARE MAMMALIAN CELLS USING PHOTODEGRADABLE HYDROGELS IN A MICROFLUIDIC PLATFORM, June 2, 2016.

(67) Kloxin, A. M.; Tibbitt, M. W.; Kasko, A. M.; Fairbairn, J. A.; Anseth, K. S. Tunable Hydrogels for External Manipulation of Cellular Microenvironments through Controlled Photodegradation. *Adv. Mater.* **2010**, *22* (1), 61–66. https://doi.org/10.1002/adma.200900917.

(68) Shenoy, R.; Tibbitt, M. W.; Anseth, K. S.; Bowman, C. N. Formation of Core–Shell Particles by Interfacial Radical Polymerization Initiated by a Glucose Oxidase-Mediated Redox System. *Chem. Mater.* **2013**, *25* (5), 761–767. https://doi.org/10.1021/cm303913f.

(69) Lewis, K. J. R.; Tibbitt, M. W.; Zhao, Y.; Branchfield, K.; Sun, X.; Balasubramaniam, V.; Anseth, K. S. In Vitro Model Alveoli from Photodegradable Microsphere Templates. *Biomater. Sci.* **2015**, *3* (6), 821–832. https://doi.org/10.1039/C5BM00034C.

(70) Kloxin, A. M.; Lewis, K. J. R.; DeForest, C. A.; Seedorf, G.; Tibbitt, M. W.; Balasubramaniam, V.; Anseth, K. S. Responsive Culture Platform to Examine the Influence of Microenvironmental Geometry on Cell Function in 3D. *Integr. Biol.* **2012**, *4* (12), 1540. https://doi.org/10.1039/c2ib20212c.

(71) McKinnon, D. D.; Brown, T. E.; Kyburz, K. A.; Kiyotake, E.; Anseth, K. S. Design and Characterization of a Synthetically Accessible, Photodegradable Hydrogel for User-Directed Formation of Neural Networks. *Biomacromolecules* **2014**, *15* (7), 2808–2816. https://doi.org/10.1021/bm500731b.